Homogenized models of conduction-advection-radiation heat transfer in porous media

Tien Dung Le, Christian Moyne, M. Sans

Homogenized models of conduction-advection-radiation heat transfer in porous media

T. D. Le[a], C. Moyne[a], M. Sans[a]

[a] *University of Lorraine, CNRS, LEMTA, F-54000 Nancy, France*

Abstract

Upscaled models are derived from the periodic homogenization technique for conduction-convection-radiation problem in porous media for the case of an opaque solid and transparent fluid. Thermal radiation at the pore-scale level is first described through a differential view factor between elementary surfaces. Such heat transfer mode is coupled with the conduction-convection mechanisms by a radiative flux in the fluid phase and a jump of conductive fluxes at the solid/fluid interface. In the framework of the periodic homogenization procedure, a macroscopic model is built with upscaled effective coefficients. Both cases of closed and open pores are studied. In the second case the radiative transfer cannot be restricted to the central unit cell. The radiation at the macroscale only affects the effective conductivity. The validity of the approach is illustrated by some simple examples. The main objective of this work is to establish the macroscopic equation form of the conduction-convection-radiation problem and to understand how the radiation affects the macroscopic behavior.

Keywords: Conduction-advection-radiation, Homogenization procedure, Macroscopic model

1. Introduction

Porous media are widely used in thermal engineering applications such as volumetric solar absorbers [1], heat exchangers [2], gas-phase heat recovery [3], porous burners [4] or insulators [5]. Such interest is justified by numerous remarkable thermal, mechanical, geometrical and optical properties and by improved manufacturing processes of a wide diversity of materials. Their heterogeneous nature allows the coupling between different modes of heat transfer such as convection, advection,

Email addresses: tien-dung.le@univ-lorraine.fr (T. D. Le), christian.moyne@univ-lorraine.fr (C. Moyne), morgansans@hotmail.fr (M. Sans)

conduction in the fluid/solid phases and radiation. The optimization of the systems where they are used necessarily requires a better understanding of the link between structural parameters of heterogeneous structures and the coupled heat transfer mechanisms [6, 1]. This can be achieved through the deployment of efficient theoretical, numerical and experimental tools.

Solving combined heat transfer on three-dimensional and complex geometries is particularly tricky and cost consuming. Hence, it is very common practice to simplify the thermal problem by considering a homogeneous equivalent medium. A unique Equivalent Thermal Conductivity (ETC), which represents the overall thermal transport, is defined and has to be identified. In this framework, the interested reader can refer to the review of Ranut [7], which provides a general overview of the studied geometries, considered thermal transfers and their scope of validity at ambient temperature. In the simplest cases, analytical or semi-analytical solutions are provided for closed structure [8, 9] and for open-cell medium [10, 11, 12, 13]. For more complex heterogeneous geometries, experiments using for example guarded hot plane [14], transient plan source [1] or flash method [15] were performed and followed by an identification procedure. These studies have allowed to investigate the validity of simplified models, the numerical or experimental characterization procedure and to quantify the influence of structural parameters on the overall heat transport.

Applications often involve high temperatures, where radiative transfer plays a leading role. Nevertheless, characterization of the equivalent radiative behavior of heterogeneous media has often been performed independently of other heat transfer modes. Monte Carlo Methods, projection methods or analytical methods were performed to identify equivalent radiative properties for structures of interest [16, 17]. Considering both conductive and radiative transfers, very few studies proposed a numerical procedure to identify equivalent properties of the porous medium. This can be explained by the difficulty to reach a sufficiently finely resolved geometry and requires efficient solvers for both modes of heat transfer [18, 19]. Recently, Mendes et al. [20, 21] or Patel et al. [22] developed a numerical hot-guarded plate method to investigate the validity of simplified radiative modelling such as the Rosseland's approximation or the assumption of equivalent homogeneous medium. More recently, Vignoles [23] and Sans et al. [24] proposed stochastic approaches to identify total equivalent diffusivity of heterogeneous structures such as ceramic, metallic foams and fibers. Luo et al. [25] analyzed the ETC of porous materials at the pore level using a discrete

ordinate ray-tracing for the radiation combined with a finite volume method to solve the energy balance equation including heat conduction.

To our knowledge, no studies are dedicated to ETC estimations of heterogeneous structures for combined conductive, radiative and advective heat transfers. Experimentally, most studies were carried out at ambient temperature on packed sphere [26, 27] or on metal foams [28, 29, 30]. High temperatures measurements remain an unsolved problem and an interesting scientific challenge. Numerically, characterization of equivalent thermal behaviour of each transport mode are performed separately. Depending on the applications, direct model of the equivalent homogeneous structure are often based on correlations obtained on a specifically developed bench [31]. Very recently, some authors like Ibarrart et al. [19] or Ma et al. [32] provided new efficient tools to simulate combined heat transfers on the heterogeneous structure but these studies were not particularly focused on ETC identification.

In this context, upscaling techniques such as the homogenization technique, the volume averaging method or the multiscale expansion method can provide a practical tool for identifying the ETC for a given heterogeneous structure. Most studies have focused on thermal dispersion, i.e., the coupling between conduction and convection through the fluid phase (see, for example, [33]). Only Whitaker [34] has studied by volume averaging the coupling between conductive and radiative heat transfer for a transparent gas phase and an opaque solid phase. To our knowledge no study has used a scaling technique to describe the simultaneous conductive, convective and radiative transport through a porous medium.

This work aims to employ the homogenization technique in the sense of [35, 33] to obtain a macroscopic law for combined conduction/advection and radiation in heterogeneous medium. We first detail the methodology associated to such homogenization techniques in the simplified case of the combined conduction and radiation within enclosed cavities with opaque interfaces. The approach is validated on two benchmark cases. Then, the model is extended to continuous pore network i.e. open cavities. Finally, adding heat transport through the fluid phase, a full combined model, which consider conduction, advection and radiation is proposed. Results of this new proposed approach are compared to solutions obtained from a computational fluid dynamic commercial software in the case of a three-dimensional simple geometry.

2. Homogenization of radiation-conduction heat transfer for disconnected closed-pores medium

2.1. Radiation in a closed-pore

Let consider a closed-inclusion with gray diffuse surface $\mathcal{S}$ of emissivity ϵ. The cavity is occupied by a transparent gas (air for example). The incident flux per unit area H_1 at the point M_1 on the surface $\mathcal{S}_1$ is given as a function of the apparent emittance (or radiosity) B_2 at the point M_2 of the surface $\mathcal{S}_2$

$$H_1 \mathrm{d}S_1 = \int_{S_2=\mathcal{S}} \mathrm{d}F_{\mathrm{d}S_2 \to \mathrm{d}S_1} B_2 \, \mathrm{d}S_2 = \int_{S_2=\mathcal{S}} \mathrm{d}F_{\mathrm{d}S_1 \to \mathrm{d}S_2} B_2 \, \mathrm{d}S_1 \tag{1}$$

where $\mathrm{d}F_{\mathrm{d}S_1 \to \mathrm{d}S_2}$ denotes the differential view factor of a radiation which leaves the elementary surface $\mathrm{d}S_1$ for arriving at $\mathrm{d}S_2$, satisfying the reciprocal relationship $\mathrm{d}S_1 \, \mathrm{d}F_{\mathrm{d}S_1 \to \mathrm{d}S_2} = \mathrm{d}S_2 \, \mathrm{d}F_{\mathrm{d}S_2 \to \mathrm{d}S_1}$. The incident flux on the surface is thus given by

$$H_1 = \int_{S_2=\mathcal{S}} \mathrm{d}F_{\mathrm{d}S_1 \to \mathrm{d}S_2} B_2 \equiv \left\{B\right\}_F\big|_1 \tag{2}$$

where $\left\{B\right\}_F\big|_1$ is an average radiosity of the inclusion weighed by the differential view factor seen from the point M_1. It should be noted that if the surface is closed

$$\int_{\mathcal{S}_2=S} \mathrm{d}F_{\mathrm{d}S_1 \to \mathrm{d}S_2} = 1 \tag{3}$$

Following the Stefan–Boltzmann law and considering the definition (2), the radiative balance on the surface allows writing the radiosity in the form

$$B_1 \;=\; \epsilon\sigma T_1^4 + (1-\epsilon) H_1 = \epsilon\sigma T_1^4 + (1-\epsilon)\left\{B\right\}_F\big|_1 = \epsilon\sigma T_1^4 + (1-\epsilon)\int_{S_2=\mathcal{S}} \mathrm{d}F_{\mathrm{d}S_1 \to \mathrm{d}S_2} B_2 \tag{4}$$

where σ is the Stefan-Boltzmann constant and T_1 the temperature at point M_1.

The heat flux lost per unit area q_1 at M_1 is defined as the difference between the radiosity and the incident flux

$$q_1 = B_1 - H_1 = B_1 - \left\{B\right\}_F\big|_1 = \epsilon\left(\sigma T_1^4 - H_1\right) = \epsilon\left(\sigma T_1^4 - \left\{B\right\}_F\big|_1\right) \tag{5}$$

which must satisfy the following condition for a closed-surface

$$\int_{S_1=\mathcal{S}} q_1 \mathrm{d}S_1 = \int_{S_1=\mathcal{S}} \left(B_1 - \left\{B\right\}_F\big|_1\right) \mathrm{d}S_1 = 0 \tag{6}$$

This relation is easily verified using the reciprocal relationship of the view factors as

$$\begin{aligned}\int_{S_1=\mathcal{S}} \{B\}_F|_1 \,\mathrm{d}S_1 &= \int_{S_1=\mathcal{S}} \mathrm{d}S_1 \int_{S_2=\mathcal{S}} B_2 \,\mathrm{d}F_{\mathrm{d}S_1\to\mathrm{d}S_2} = \int_{S_1=\mathcal{S}} \int_{S_2=\mathcal{S}} B_2 \,\mathrm{d}F_{\mathrm{d}S_2\to\mathrm{d}S_1}\mathrm{d}S_2 \\ &= \int_{S_2=\mathcal{S}} B_2 \,\mathrm{d}S_2 \int_{S_1=\mathcal{S}} \mathrm{d}F_{\mathrm{d}S_2\to\mathrm{d}S_1} = \int_{S_2=\mathcal{S}} B_2 \,\mathrm{d}S_2 = |\mathcal{S}|\,\{B\}_S \end{aligned} \tag{7}$$

by noting $\{B\}_S$ the surface average radiosity. Note that relation (7) is valid regardless of the quantity B varying over the $\mathcal{S}$ surface of the inclusion.

2.2. Homogenization procedure

We now apply the periodic homogenization technique to obtain the macroscopic laws for the coupled conduction-radiation problem. The porous medium is composed of a solid phase occupied by the volume V_s and disconnected closed-pores of volume V_f containing a transparent fluid, with the solid/pore interface A_{fs}. In this context, the radiation within the fluid phase and the conduction mechanism in both phases are considered leading to the pore-scale model as follows

$$\left\{\begin{array}{rcll} (\rho c)_f \dfrac{\partial T_f}{\partial t} &=& \boldsymbol{\nabla}\cdot\left(\lambda_f \boldsymbol{\nabla} T_f - \mathbf{q}^{\mathrm{R}}\right) & \text{in } V_f \\ (\rho c)_s \dfrac{\partial T_s}{\partial t} &=& \boldsymbol{\nabla}\cdot\left(\lambda_s \boldsymbol{\nabla} T_s\right) & \text{in } V_s \\ T_f &=& T_s & \text{on } A_{fs} \\ -\lambda_f \boldsymbol{\nabla} T_f\cdot\mathbf{n}_f - \lambda_s \boldsymbol{\nabla} T_s\cdot\mathbf{n}_s &=& -\mathbf{q}^{\mathrm{R}}\cdot\mathbf{n}_f & \\ \mathbf{q}^{\mathrm{R}}\cdot\mathbf{n}_f &=& -(B-\{B\}_F) & \end{array}\right. \tag{8}$$

where $\mathbf{q}^{\mathrm{R}}$ is the radiative flux in the fluid phase. $(\rho c)_i$ and λ_i represent the volumetric heat capacity and conductivity of the phase i ($i = f, s$ refers to fluid or solid phases). $\mathbf{n}_i$ is the unit normal vector at the solid/fluid interface outward to the phase i. The radiosity B given by (4) is solution of the integral equation on the interface $\mathcal{S}$ of the closed inclusion

$$B = \epsilon\sigma T^4 + (1-\epsilon)\int_{S_1=\mathcal{S}} \mathrm{d}F_{\mathrm{d}S\to\mathrm{d}S_1} B_1 = \epsilon\sigma T^4 + (1-\epsilon)\,\{B\}_F \tag{9}$$

where the view factor average operator is defined as:

$$\{f\}_F = \int_{S_1=\mathcal{S}} \mathrm{d}F_{\mathrm{d}S\to\mathrm{d}S_1} f \tag{10}$$

The above equation system is supplemented by boundary conditions on the external boundary and the temperature field at the initial time.

The medium is characterized by a periodic Representative Elementary Volume (REV) Y of size ℓ, composed of a fluid phase Y_f and a solid phase Y_s with an interface ∂Y_{fs}. The space is separated into two different spatial scales: the microscopic scale of characterized length ℓ and the macroscopic scale of length L where $\eta = \ell/L$ is a small perturbation parameter. A dimensional analysis is firstly carried out to construct the η-microscopic model. The reference time can be chosen as the characteristic conductive time at the macroscale of the solid phase, $t^{\text{ref}} = L^2/a_s$ where $a_{s(f)} = \lambda_{s(f)}/(\rho c)_{s(f)}$ is the thermal diffusivity of the solid (fluid) phase. As a macroscopic point of view is adopted, the reference length is chosen to be the macroscopic length L. The dimensionless quantities are indexed with *. Finally, the set of dimensionless equations is written as

$$\left\{\begin{array}{rcll} \dfrac{a_s}{a_f}\dfrac{\partial T_f^*}{\partial t^*} & = & \nabla^{*2} T_f^* - \dfrac{L q^{\text{R,ref}}}{\lambda_f T^{\text{ref}}} \boldsymbol{\nabla}^* \cdot \mathbf{q}^{\text{R}^*} & \text{in } Y_f \\ \dfrac{\partial T_s^*}{\partial t^*} & = & \nabla^{*2} T_s^* & \text{in } Y_s \\ T_f^* & = & T_s^* & \text{on } \partial Y_{fs} \\ -\boldsymbol{\nabla}^* T_f^* \cdot \mathbf{n}_f - \dfrac{\lambda_s}{\lambda_f} \boldsymbol{\nabla}^* T_s^* \cdot \mathbf{n}_s & = & -\dfrac{L q^{\text{R,ref}}}{\lambda_f T^{\text{ref}}} \mathbf{q}^{\text{R}^*} \cdot \mathbf{n}_f & \\ \mathbf{q}^{\text{R}^*} \cdot \mathbf{n}_f & = & -\dfrac{B^{\text{ref}}}{q^{\text{R,ref}}} \left(B^* - \{B\}_F^*\right) & \end{array}\right. \tag{11}$$

where $q^{\text{R,ref}}$, B^{ref} and T^{ref} are the reference quantities of the radiative heat flux, radiosity and temperature.

The most interesting case to observe the radiation impact on the conduction problem is the case when the radiative flux is of the same order of magnitude as the conductive heat flux in the fluid phase at the macroscale, i.e. $q^{\text{R,ref}} = \mathcal{O}(\lambda_f T^{\text{ref}}/L)$. On the other hand, at the pore-scale, the radiosity B and the conductive flux at the solid/fluid interface should be of the same order of magnitude yielding $B^{\text{ref}} = \mathcal{O}(\lambda_f T^{\text{ref}}/\ell)$ leading to $B^{\text{ref}}/q^{\text{R,ref}} = \mathcal{O}(\eta^{-1})$. If the order of magnitude of the radiative term is lower than the conductive one, the radiation is dominated by the conduction and therefore can be ignored in Eq. (11). Moreover, the predominant radiation case can also be treated by the same approach as demonstrated at the end of this section.

It will be assumed that $a_s/a_f = \mathcal{O}(1)$ and $\lambda_s/\lambda_f = \mathcal{O}(1)$. The system (11) becomes

$$\left\{\begin{array}{rcll} \dfrac{a_s}{a_f}\dfrac{\partial T_f^*}{\partial t^*} & = & \nabla^{*2} T_f^* - \boldsymbol{\nabla}^* \cdot \mathbf{q}^{\mathrm{R}^*} & \text{in } Y_f \\ \dfrac{\partial T_s^*}{\partial t^*} & = & \nabla^{*2} T_s^* & \text{in } Y_s \\ T_f^* & = & T_s^* & \text{on } \partial Y_{fs} \\ -\boldsymbol{\nabla}^* T_f^* \cdot \mathbf{n}_f - \boldsymbol{\nabla}^* T_s^* \cdot \mathbf{n}_s & = & -\mathbf{q}^{\mathrm{R}^*} \cdot \mathbf{n}_f & \\ \mathbf{q}^{\mathrm{R}^*} \cdot \mathbf{n}_f & = & -\dfrac{1}{\eta}\left(B^* - \{B\}_F^*\right) & \end{array}\right. \tag{12}$$

The temperature T is function of the two separated space variables: macroscopic (or slow) variable $\mathbf{x}$ associated with the length scale L ($\mathbf{x}^* = \mathbf{x}/L = \mathcal{O}(\mathbf{1})$) and microscopic (or fast) variable $\mathbf{y}$ associated with ℓ ($\mathbf{y}^* = \mathbf{y}/\ell = \mathcal{O}(\mathbf{1})$). The space derivative operator is given by

$$\boldsymbol{\nabla}^* = L\boldsymbol{\nabla} = L\left(\boldsymbol{\nabla}_x + \boldsymbol{\nabla}_y\right) = L\left(\frac{1}{L}\boldsymbol{\nabla}_{x^*} + \frac{1}{\ell}\boldsymbol{\nabla}_{y^*}\right) = \boldsymbol{\nabla}_{x^*} + \frac{1}{\eta}\boldsymbol{\nabla}_{y^*} \tag{13}$$

The problem is finally rewritten in dimensional form by formally keeping the η factor to indicate the order of magnitude of the different terms in a Y unit-cell, yielding the η-microscopic model

$$\left\{\begin{array}{rcll} (\rho c)_f \dfrac{\partial T_f}{\partial t} & = & \boldsymbol{\nabla} \cdot \left(\lambda_f \boldsymbol{\nabla} T_f - \mathbf{q}^{\mathrm{R}}\right) & \text{in } Y_f \\ (\rho c)_s \dfrac{\partial T_s}{\partial t} & = & \boldsymbol{\nabla} \cdot \left(\lambda_s \boldsymbol{\nabla} T_s\right) & \text{in } Y_s \\ T_f & = & T_s & \text{on } \partial Y_{fs} \\ -\lambda_f \boldsymbol{\nabla} T_f \cdot \mathbf{n}_f - \lambda_s \boldsymbol{\nabla} T_s \cdot \mathbf{n}_s & = & -\mathbf{q}^{\mathrm{R}} \cdot \mathbf{n}_f & \\ \mathbf{q}^{\mathrm{R}} \cdot \mathbf{n}_f & = & -\dfrac{1}{\eta}\left(B - \{B\}_F\right) & \end{array}\right. \tag{14}$$

with $\boldsymbol{\nabla} = \frac{1}{\eta}\boldsymbol{\nabla}_y + \boldsymbol{\nabla}_x$. In the framework of the homogenization technique, the temperatures are sought in the form of a series expansion of the small parameter η

$$\begin{array}{rcl} T_f(t,\mathbf{x},\mathbf{y}) & = & \displaystyle\sum_{k=0}^{\infty} \eta^k\, T_f^{(k)}(t,\mathbf{x},\mathbf{y}) \\ T_s(t,\mathbf{x},\mathbf{y}) & = & \displaystyle\sum_{k=0}^{\infty} \eta^k\, T_s^{(k)}(t,\mathbf{x},\mathbf{y}) \end{array} \tag{15}$$

where $T_f^{(k)}(t,\mathbf{x},\mathbf{y})$ and $T_s^{(k)}(t,\mathbf{x},\mathbf{y})$ are $\mathbf{y}$-periodic functions. The successive problems for the different orders of $T_f^{(k)}$ and $T_s^{(k)}$ for $k = 1, 2, \ldots$ will be then collected. In a similar fashion, the radiosity B is also decomposed in a series expansion as

$$B(t,\mathbf{x},\mathbf{y}) = \sum_{k=0}^{\infty} \eta^k\, B^{(k)}(t,\mathbf{x},\mathbf{y}) \tag{16}$$

Inserting (15) and (16) in (9) yields

$$\sum_k \eta^k B^{(k)}(t,\mathbf{x},\mathbf{y}) = \epsilon\sigma\left(\sum_k \eta^k T^{(k)}(t,\mathbf{x},\mathbf{y})\right)^4 + (1-\epsilon)\sum_k \eta^k \int_{S_2=\mathcal{S}} \mathrm{d}F_{\mathrm{d}S\to\mathrm{d}S_2} B_2^{(k)}(t,\mathbf{x},\mathbf{y}) \quad (17)$$

- **Problem for $T^{(0)}$**

The problem for $T^{(0)}$ at the order $\mathcal{O}(\eta^{-2})$ is written as

$$\left\{\begin{array}{rcll} 0 &=& \boldsymbol{\nabla}_y\cdot\left(\lambda_f\boldsymbol{\nabla}_y T_f^{(0)}\right) & \text{in } Y_f \\ 0 &=& \boldsymbol{\nabla}_y\cdot\left(\lambda_s\boldsymbol{\nabla}_y T_s^{(0)}\right) & \text{in } Y_s \\ T_f^{(0)} &=& T_s^{(0)} & \text{on } \partial Y_{fs} \\ -\mathbf{q}^{R(-1)}\cdot\mathbf{n}_f &=& -\lambda_f\boldsymbol{\nabla}_y T_f^{(0)}\cdot\mathbf{n}_f - \lambda_s\boldsymbol{\nabla}_y T_s^{(0)}\cdot\mathbf{n}_s & \\ \mathbf{q}^{R(-1)}\cdot\mathbf{n}_f &=& -\left(B^{(0)} - \{B^{(0)}\}_F\right) & \\ B^{(0)} &=& \epsilon\sigma {T^{(0)}}^4 + (1-\epsilon)\{B^{(0)}\}_F & \\ \text{and}\quad \left\{B^{(0)}\right\}_F &=& \displaystyle\int_{S_1=\partial Y_{fs}} \mathrm{d}F_{\mathrm{d}S\to\mathrm{d}S_1} B_1^{(0)}\,. & \end{array}\right. \quad (18)$$

The solution of the preceding problem is $T_f^{(0)}(t,\mathbf{x},\mathbf{y}) = T_s^{(0)}(t,\mathbf{x},\mathbf{y}) \equiv T^{(0)}(t,\mathbf{x})$, $B^{(0)} = \left\{B^{(0)}\right\}_F = \sigma {T^{(0)}}^4(t,\mathbf{x})$ and $\mathbf{q}^{R(-1)}\cdot\mathbf{n}_f = 0$.

- **Problem for $T^{(1)}$**

The problem for $T^{(1)}$ at the order $\mathcal{O}(\eta^{-1})$ is written as

$$\left\{\begin{array}{rcll} 0 &=& \boldsymbol{\nabla}_y\cdot\left(\lambda_f\boldsymbol{\nabla}_y T_f^{(1)}\right) - \boldsymbol{\nabla}_y\cdot\mathbf{q}^{\mathrm{R}(0)} & \text{in } Y_f \\ 0 &=& \boldsymbol{\nabla}_y\cdot\left(\lambda_s\boldsymbol{\nabla}_y T_s^{(1)}\right) & \text{in } Y_s \\ T_f^{(1)} &=& T_s^{(1)} & \text{on } \partial Y_{fs} \\ -\mathbf{q}^{\mathrm{R}(0)}\cdot\mathbf{n}_f &=& -\lambda_f\left(\boldsymbol{\nabla}_y T_f^{(1)} + \boldsymbol{\nabla}_x T^{(0)}\right)\cdot\mathbf{n}_f - \lambda_s\left(\boldsymbol{\nabla}_y T_s^{(1)} + \boldsymbol{\nabla}_x T^{(0)}\right)\cdot\mathbf{n}_s & \end{array}\right. \quad (19)$$

It should be noted that the radiative flux is not absorbed by the transparent fluid phase leading to $\boldsymbol{\nabla}_y\cdot\mathbf{q}^{\mathrm{R}(0)} = 0$ in the fluid phase Y_f. The solution is sought in the form

$$\begin{array}{rcll} T_f^{(1)}(t,\mathbf{x},\mathbf{y}) &=& \boldsymbol{\chi}_f(\mathbf{y})\cdot\boldsymbol{\nabla}_x T^{(0)}(t,\mathbf{x}) + \widehat{T}^{(1)}(t,\mathbf{x}) & \text{in } Y_f \\ T_s^{(1)}(t,\mathbf{x},\mathbf{y}) &=& \boldsymbol{\chi}_s(\mathbf{y})\cdot\boldsymbol{\nabla}_x T^{(0)}(t,\mathbf{x}) + \widehat{T}^{(1)}(t,\mathbf{x}) & \text{in } Y_s \end{array} \quad (20)$$

where $\widehat{T}^{(1)}(t,\mathbf{x})$ plays the role of an integration constant. From (17), the problem in $B^{(1)}$ is written as

$$\begin{aligned}\sigma {T^{(0)}}^4(t,\mathbf{x})+\eta B^{(1)} &= \epsilon\sigma\left[{T^{(0)}}^4(t,\mathbf{x})+4\eta {T^{(0)}}^3 T^{(1)}\right]\\ &\quad +(1-\epsilon)\int_{S_1=\partial Y_{fs}} \mathrm{d}F_{\mathrm{d}S\to\mathrm{d}S_1}\left[\sigma {T_1^{(0)}}^4(t,\mathbf{x})+\eta B_1^{(1)}\right]+\mathcal{O}(\eta^2) \qquad (21)\end{aligned}$$

To compute the radiative transfer through the fluid phase, a precise evaluation of the local temperature in the unit cell at the order $\mathcal{O}(\eta)$ is needed. Denoting by 0 the origin of the $\mathbf{y}$-axis in the unit cell ($\mathbf{y}=\mathbf{x}-\mathbf{x}_0$), a Taylor development gives

$$T^{(0)}(t,\mathbf{x}) = T^{(0)}(t,\mathbf{x}_0)+\eta\mathbf{y}\cdot\boldsymbol{\nabla}_x T^{(0)}+\mathcal{O}(\eta^2) \qquad (22)$$

Noting that $\boldsymbol{\nabla}_x T^{(0)}$ can be considered constant in the unit cell and the above equation is correct at order $\mathcal{O}(\eta^2)$. Therefore, by inserting (22) in (21) and noting that the first order terms $\sigma {T^{(0)}}^4(\mathbf{x}_0)$ cancel out, the equation for $B^{(1)}$ reads as

$$\begin{aligned}B^{(1)}+4(1-\epsilon)\sigma {T^{(0)}}^3\mathbf{y}\cdot\boldsymbol{\nabla}_x T^{(0)} &= 4\epsilon\sigma {T^{(0)}}^3 T^{(1)}\\ &+ (1-\epsilon)\int_{S_1=\partial Y_{fs}} \mathrm{d}F_{\mathrm{d}S\to\mathrm{d}S_1}\left(4\sigma {T^{(0)}}^3\mathbf{y}_1\boldsymbol{\nabla}_x T^{(0)}+B_1^{(1)}\right) \qquad (23)\end{aligned}$$

Using the closure (20) for $T^{(1)}$ with $\boldsymbol{\chi}\equiv\boldsymbol{\chi}_f=\boldsymbol{\chi}_s$ on the solid/fluid interface ∂Y_{fs}, the solution for $B^{(1)}$ is searched in the form

$$B^{(1)}(t,\mathbf{x},\mathbf{y}) = 4\sigma {T^{(0)}}^3(t,\mathbf{x})\left[\widehat{T}^{(1)}(t,\mathbf{x})+\boldsymbol{\beta}(\mathbf{y})\cdot\boldsymbol{\nabla}_x T^{(0)}(t,\mathbf{x})\right] \qquad (24)$$

The vector $\boldsymbol{\beta}(\mathbf{y})$ satisfies

$$\begin{aligned}\boldsymbol{\beta}+(1-\epsilon)\mathbf{y} &= \epsilon\boldsymbol{\chi}+(1-\epsilon)\int_{S_1=\partial Y_{fs}}\mathrm{d}F_{\mathrm{d}S\to\mathrm{d}S_1}\left(\boldsymbol{\beta}_1+\mathbf{y}_1\right)\\ &= \epsilon\boldsymbol{\chi}+(1-\epsilon)\left\{\boldsymbol{\beta}+\mathbf{y}\right\}_F \qquad (25)\end{aligned}$$

where $\{\boldsymbol{\beta}\}_F$ is the view factor average of $\boldsymbol{\beta}$ defined in (10). $\boldsymbol{\chi}$ and $\boldsymbol{\beta}$ are defined to within one additive constant that plays no role since only the quantity $\boldsymbol{\beta}-\{\boldsymbol{\beta}\}_F$ appears in the boundary condition on the interface ∂Y_{fs}. It can be noted that the problem (25) is independent on the origin of the $\mathbf{y}$ vector. For the particular case of a black cavity with $\epsilon=1$, the solution of the integral equation (25) is: $\boldsymbol{\beta}=\boldsymbol{\chi}$.

The radiative flux on the fluid-solid interface is given by

$$\begin{aligned}\mathbf{q}^{\mathrm{R}(0)}\cdot\mathbf{n}_f &= 4\sigma {T^{(0)}}^3\left(\{\mathbf{y}\}_F-\mathbf{y}\right)\cdot\boldsymbol{\nabla}_x T^{(0)}+\{B^{(1)}\}_F-B^{(1)}\\ &= 4\sigma {T^{(0)}}^3\left[\{\mathbf{y}+\boldsymbol{\beta}\}_F-(\mathbf{y}+\boldsymbol{\beta})\right]\cdot\boldsymbol{\nabla}_x T^{(0)}\end{aligned}\tag{26}$$

From (19), (20) and (24), the vectors $\boldsymbol{\chi}_f(\mathbf{y})$ and $\boldsymbol{\chi}_s(\mathbf{y})$ are solution of the following problem

$$\left\{\begin{array}{rcll} 0 &=& \boldsymbol{\nabla}_y\cdot\left(\lambda_f\boldsymbol{\nabla}_y\boldsymbol{\chi}_f\right) & \text{in } Y_f\\ 0 &=& \boldsymbol{\nabla}_y\cdot\left(\lambda_s\boldsymbol{\nabla}_y\boldsymbol{\chi}_s\right) & \\ \boldsymbol{\chi}_f &=& \boldsymbol{\chi}_s & \text{on } \partial Y_{fs}\\ -\lambda_f\mathbf{n}_f\cdot\left(\boldsymbol{\nabla}_y\boldsymbol{\chi}_f+\boldsymbol{I}\right)-\lambda_s\mathbf{n}_s\cdot\left(\boldsymbol{\nabla}_y\boldsymbol{\chi}_s+\boldsymbol{I}\right) &=& 4\sigma {T^{(0)}}^3\left(\mathbf{y}+\boldsymbol{\beta}-\{\mathbf{y}+\boldsymbol{\beta}\}_F\right) & \end{array}\right.\tag{27}$$

where the vector $\boldsymbol{\beta}$ is the solution of the integral equation (25). Thanks to the relation (7), it is immediate to verify that the surface integral of the radiative source term in (27) vanishes in the unit cell, which is a necessary condition to have a solution for $\boldsymbol{\chi}_f$ and $\boldsymbol{\chi}_s$.

- **Problem for $T^{(2)}$**

The problem in $T^{(2)}$ at the order $\mathcal{O}(\eta^0)$ is given as

$$\left\{\begin{array}{rcll} (\rho c)_f\dfrac{\partial T^{(0)}}{\partial t} &=& \boldsymbol{\nabla}_y\cdot\left[\lambda_f\left(\boldsymbol{\nabla}_y T_f^{(2)}+\boldsymbol{\nabla}_x T_f^{(1)}\right)-\mathbf{q}^{\mathrm{R}(1)}\right] & \\ &+& \boldsymbol{\nabla}_x\cdot\left[\lambda_f\left(\boldsymbol{\nabla}_y T_f^{(1)}+\boldsymbol{\nabla}_x T^{(0)}\right)-\mathbf{q}^{\mathrm{R}(0)}\right] & \text{in } Y_f\\ (\rho c)_s\dfrac{\partial T^{(0)}}{\partial t} &=& \boldsymbol{\nabla}_y\cdot\left[\lambda_s\left(\boldsymbol{\nabla}_y T_s^{(2)}+\boldsymbol{\nabla}_x T_s^{(1)}\right)\right]+\boldsymbol{\nabla}_x\cdot\left[\lambda_s\left(\boldsymbol{\nabla}_y T_s^{(1)}+\boldsymbol{\nabla}_x T^{(0)}\right)\right] & \text{in } Y_s\\ -\mathbf{q}^{\mathrm{R}(1)}\cdot\mathbf{n}_f &=& -\lambda_f\left(\boldsymbol{\nabla}_y T_f^{(2)}+\boldsymbol{\nabla}_x T_f^{(1)}\right)\cdot\mathbf{n}_f-\lambda_s\left(\boldsymbol{\nabla}_y T_s^{(2)}+\boldsymbol{\nabla}_x T_s^{(1)}\right)\cdot\mathbf{n}_s & \text{on } \partial Y_{fs}\end{array}\right.\tag{28}$$

The intrinsic phase averages $\langle\ \rangle^{f(s)}$ over the unit cell are classically defined by

$$\langle\ \rangle^{f(s)}=\frac{1}{|Y_{f(s)}|}\int_{Y_{f(s)}}\mathrm{d}V\tag{29}$$

By using the divergence theorem, the interface condition (28c) and solutions (20), equations (28a) and (28b) are averaged over the unit cell and then added leading to

$$\langle\rho c\rangle\frac{\partial T^{(0)}}{\partial t}=\boldsymbol{\nabla}_x\cdot\left\{\left[n_f\lambda_f(\boldsymbol{I}+\left\langle\boldsymbol{\nabla}_y\boldsymbol{\chi}_f\right\rangle^f)+n_s\lambda_s(\boldsymbol{I}+\langle\boldsymbol{\nabla}_y\boldsymbol{\chi}_s\rangle^s)\right]\cdot\boldsymbol{\nabla}_x T^0-\left\langle\mathbf{q}^{\mathrm{R}(0)}\right\rangle\right\}\tag{30}$$

where $n_{f(s)}=|Y_{f(s)}|/|Y|$ is the fluid (solid) volume fraction and $\langle\rho c)\rangle=n_f(\rho c)^f+n_s(\rho c)^s$. It remains to calculate $\left\langle\mathbf{q}^{\mathrm{R}(0)}\right\rangle$. It should be kept in mind that as the fluid phase is transparent, $\boldsymbol{\nabla}_y\cdot\mathbf{q}_f^{\mathrm{R}(0)}=0$ in the fluid phase. Let consider the identity

$$\boldsymbol{\nabla}_y\cdot\left(\mathbf{q}_f^{\mathrm{R}(0)}\otimes\mathbf{y}\right)=\mathbf{q}_f^{\mathrm{R}(0)}+\boldsymbol{\nabla}_y\cdot\mathbf{q}_f^{\mathrm{R}(0)}\ \mathbf{y}=\mathbf{q}_f^{\mathrm{R}(0)}\tag{31}$$

By using relation (26), we obtain

$$\begin{aligned}\left\langle \mathbf{q}_f^{\mathrm{R}(0)} \right\rangle &= \frac{1}{|Y|}\int_{Y_f} \boldsymbol{\nabla}_y \cdot \left(\mathbf{q}_f^{\mathrm{R}(0)} \otimes \mathbf{y}\right) \mathrm{d}V = \frac{1}{|Y|}\int_{\partial Y_{fs}} \mathbf{y}\left(\mathbf{q}_f^{\mathrm{R}(0)} \cdot \mathbf{n}_f\right) \mathrm{d}S \\ &= \frac{4\sigma {T^{(0)}}^3}{|Y|}\int_{\partial Y_{fs}} \mathbf{y} \otimes \left(\{\mathbf{y}+\boldsymbol{\beta}\}_F - (\mathbf{y}+\boldsymbol{\beta})\right) \mathrm{d}S \cdot \boldsymbol{\nabla}_x T^{(0)} \end{aligned} \tag{32}$$

Finally the macroscopic equation for the conduction/radiation coupled heat transfer is written as:

$$\langle \rho c \rangle \frac{\partial T^{(0)}}{\partial t} = \boldsymbol{\nabla}_x \cdot \left(\boldsymbol{\lambda}_{eq} \cdot \boldsymbol{\nabla}_x T^0\right) \tag{33}$$

with an equivalent thermal conductivity tensor given by

$$\begin{aligned}\boldsymbol{\lambda}_{eq} &= n_f \left[\lambda_f \left(\boldsymbol{I} + \left\langle \boldsymbol{\nabla}_y \boldsymbol{\chi}_f \right\rangle^f\right) + \frac{4\sigma {T^{(0)}}^3}{|Y_f|}\int_{\partial Y_{fs}} \mathbf{y} \otimes \left(\mathbf{y} + \boldsymbol{\beta} - \{\mathbf{y}+\boldsymbol{\beta}\}_F\right) \mathrm{d}S\right] \\ &+ n_s \lambda_s \left(\boldsymbol{I} + \left\langle \boldsymbol{\nabla}_y \boldsymbol{\chi}_s \right\rangle^s\right) \end{aligned} \tag{34}$$

The classical case of pure conduction is immediately recovered neglecting the radiative part. It must be emphasized that the surface-to-surface radiation in a porous medium composed of closed pores modifies the effective conductivity and the macroscopic equation form is similar to the one of a conductive heat transfer problem.

In particular geometries as parallel solid layers or spherical pores, the equivalent thermal conductivity can be analytically evaluated as demonstrated in Appendix A.

2.3. Predominant radiation

We now consider the predominant radiation case when the order of magnitude of the radiative term is higher than the conductive one, *i.e.* $4\sigma {T^{(0)}}^3 \ell \gg \lambda_f$ or λ_s. The left-hand side of the boundary condition (27d) on the interface ∂Y_{fs} vanishes, leading to $\boldsymbol{\beta} = -\mathbf{y}$. Inserting this value of $\boldsymbol{\beta}$ into Eq. (25) gives $\boldsymbol{\chi} = -\mathbf{y}$. The problem for $\boldsymbol{\chi}$ is now written as

$$\left\{\begin{array}{rcll} 0 &=& \nabla^2 \boldsymbol{\chi}_f & \text{in } Y_f \\ 0 &=& \nabla^2 \boldsymbol{\chi}_s & \text{in } Y_s \\ \boldsymbol{\chi}_f &=& \boldsymbol{\chi}_s = -\mathbf{y} & \text{on } \partial Y_{fs} \end{array}\right. \tag{35}$$

which is a decoupled problem for $\boldsymbol{\chi}_f$ and $\boldsymbol{\chi}_s$. The solution in Y_f is $\boldsymbol{\chi}_f = -\mathbf{y}$ (the temperature inside the fluid inclusion Y_f is uniform due to high radiative effect). It remains to solve the problem

for $\boldsymbol{\chi}_s$ which depends only on the geometry. We adopt here the technique introduced by Lévy in this case [36, 37]. The time-dependent equations at $\mathcal{O}(\varepsilon^0)$ read as

$$\begin{array}{rcll} (\rho c)_f \dfrac{\partial T^{(0)}}{\partial t} & = & -\left(\boldsymbol{\nabla}_x \cdot \mathbf{q}_f^{(0)} + \boldsymbol{\nabla}_y \cdot \mathbf{q}_f^{(1)}\right) & \text{in } Y_f \\ (\rho c)_s \dfrac{\partial T^{(0)}}{\partial t} & = & -\left(\boldsymbol{\nabla}_x \cdot \mathbf{q}_s^{(0)} + \boldsymbol{\nabla}_y \cdot \mathbf{q}_s^{(1)}\right) & \text{in } Y_s \end{array} \tag{36}$$

where

$$\left\{ \begin{array}{rcl} \mathbf{q}_f^{(0)} & = & -\lambda_f \left(\boldsymbol{\nabla}_x T^{(0)} + \boldsymbol{\nabla}_y T_f^{(1)}\right) + \mathbf{q}^{R(0)} \\ \mathbf{q}_s^{(0)} & = & -\lambda_s \left(\boldsymbol{\nabla}_x T^{(0)} + \boldsymbol{\nabla}_y T_s^{(1)}\right) \\ \mathbf{q}_f^{(1)} & = & -\lambda_f \left(\boldsymbol{\nabla}_x T_f^{(1)} + \boldsymbol{\nabla}_y T_f^{(2)}\right) + \mathbf{q}^{R(1)} \\ \mathbf{q}_s^{(1)} & = & -\lambda_s \left(\boldsymbol{\nabla}_x T_s^{(1)} + \boldsymbol{\nabla}_y T_s^{(2)}\right) \end{array} \right. \tag{37}$$

Averaging (36) over the unit cell, taking into account the periodicity and the continuity of the normal fluxes ($\mathbf{q}_f^{(1)} \cdot \mathbf{n} = \mathbf{q}_s^{(1)} \cdot \mathbf{n}$ on ∂Y_{fs}) leads to

$$\langle \rho c \rangle \frac{\partial T^{(0)}}{\partial t} = -\boldsymbol{\nabla}_x \cdot \frac{1}{|Y|} \left(\int_{Y_f} \mathbf{q}_f^{(0)} \mathrm{d}V + \int_{Y_s} \mathbf{q}_s^{(0)} \mathrm{d}V \right) \tag{38}$$

As $\boldsymbol{\nabla}_y \cdot \mathbf{q}_f^{(0)} = 0$ and $\boldsymbol{\nabla}_y \cdot \mathbf{q}_s^{(0)} = 0$, we have

$$\left\{ \begin{array}{rcl} \mathbf{q}_f^{(0)} & = & \boldsymbol{\nabla}_y \cdot \left(\mathbf{q}_f^{(0)} \otimes \mathbf{y}\right) \\ \mathbf{q}_s^{(0)} & = & \boldsymbol{\nabla}_y \cdot \left(\mathbf{q}_s^{(0)} \otimes \mathbf{y}\right) \end{array} \right. \tag{39}$$

Noting that $\mathbf{q}_f^{(0)} \cdot \mathbf{n} = \mathbf{q}_s^{(0)} \cdot \mathbf{n}$ on ∂Y_{fs}, we obtain

$$\begin{array}{rcl} \langle \rho c \rangle \dfrac{\partial T^{(0)}}{\partial t} & = & -\boldsymbol{\nabla}_x \cdot \dfrac{1}{|Y|} \left[\displaystyle\int_{\partial Y_{fs}} \mathbf{n}_f \cdot \left(\mathbf{q}_f^{(0)} \otimes \mathbf{y}\right) \mathrm{d}S + \int_{\partial Y_{fs}+Y_{se}} \mathbf{n}_s \cdot \left(\mathbf{q}_s^{(0)} \otimes \mathbf{y}\right) \mathrm{d}S \right] \\ & = & -\boldsymbol{\nabla}_x \cdot \dfrac{1}{|Y|} \left[\displaystyle\int_{\partial Y_{se}} \mathbf{n}_s \cdot \left(\mathbf{q}_s^{(0)} \otimes \mathbf{y}\right) \mathrm{d}S \right] \\ & = & \boldsymbol{\nabla}_x \cdot \left[\dfrac{1}{|Y|} \left(\displaystyle\int_{\partial Y_{se}} \lambda_s \left(\mathbf{y} \otimes \mathbf{n}_s\right) \cdot \left(\boldsymbol{I} + \boldsymbol{\nabla}_y \boldsymbol{\chi}_s\right) \mathrm{d}S \right) \cdot \boldsymbol{\nabla}_x T^{(0)} \right] = \boldsymbol{\nabla}_x \cdot \left(\boldsymbol{\lambda}_{eq} \cdot \boldsymbol{\nabla}_x T^{(0)}\right) \end{array} \tag{40}$$

It is important to note that in the case of predominant radiation, the thermal conductivity of the fluid phase λ_f and the radiative terms do not appear in the final form of the equivalent conductivity $\boldsymbol{\lambda}_{eq}$.

3. Extension to the case of a continuous fluid phase

We now analyze the case of a porous medium composed of a continuous fluid phase. In this context, the main difficulty stems from the fact that while the diffusive problem can be solved in a single unit cell, radiation emitted or received by one unit cell can come from solid surfaces of adjacent unit cells. Nevertheless, it is assumed that the radiation retains a local behavior as the radiative transport occurs only between the neighboring cells close to the central cell. Therefore, the scale separation hypothesis can be verified.

3.1. Problem for $B^{(1)}$

Each unit cell is identified by an integer multi-index $\mathbf{k} \in \mathbb{Z}^3$. $\mathbf{k} = (0,0,0)$ denotes the central cell in which the calculation is made. Let define the diagonal matrix

$$\boldsymbol{L} = \begin{pmatrix} l_1 & 0 & 0 \\ 0 & l_2 & 0 \\ 0 & 0 & l_3 \end{pmatrix} \tag{41}$$

where $\ell_i, i \in \{1,2,3\}$ denotes the spatial periods corresponding to the size of the parallelepipedic unit cell in the three space directions. To simplify the notations, the variable t is omitted in this section.

The closure problem (27) for $\boldsymbol{\chi}_{f(s)}$ remains the same. However, equation (9) for the radiosity in the unit cell $\mathbf{i}$ is now written as

$$\begin{aligned} B_{\mathbf{i}}(\mathbf{x_i}+\mathbf{y},\mathbf{y}) &= \epsilon\sigma T_{\mathbf{i}}^4(\mathbf{x_i}+\mathbf{y},\mathbf{y}) + (1-\epsilon)\{B_{\mathbf{i}}\}_F \\ &= \epsilon\sigma T_{\mathbf{i}}^4(\mathbf{x_i}+\mathbf{y},\mathbf{y}) + (1-\epsilon)\sum_{\mathbf{k}\in\mathbb{Z}^3}\int_{\partial Y_{fs}} \mathrm{d}F_{\mathrm{d}S_{\mathbf{i}}\to\mathrm{d}S_{\mathbf{k}}} B_{\mathbf{k}} \end{aligned} \tag{42}$$

where $B_{\mathbf{i}}(\mathbf{x_i}+\mathbf{y},\mathbf{y})$ (or $T_{\mathbf{i}}(\mathbf{x_i}+\mathbf{y},\mathbf{y})$) denotes the radiosity (or temperature) within the unit cell $\mathbf{i}$ whose center is located at the position $\mathbf{x_i} = \mathbf{x_0} + \boldsymbol{L}\cdot\mathbf{i}$ and ∂Y_{fs} the interface fluid-solid within one cell. The coordinate $\mathbf{y}$ designates the position of the point in the cell $\mathbf{i}$ relative to the cell center $\mathbf{x_i}$. It should be noted that

$$\sum_{\mathbf{k}\in\mathbb{Z}^3}\int_{(\partial Y_{fs})_{\mathbf{i}+\mathbf{k}}} \mathrm{d}F_{\mathrm{d}S_{\mathbf{i}}\to\mathrm{d}S_{\mathbf{i}+\mathbf{k}}} = 1 \qquad \text{and} \qquad \mathrm{d}F_{\mathrm{d}S_{\mathbf{i}}\to\mathrm{d}S_{\mathbf{i}+\mathbf{k}}} = \mathrm{d}F_{\mathrm{d}S_{\mathbf{0}}\to\mathrm{d}S_{\mathbf{k}}} \tag{43}$$

so that the integration surface $\mathcal{S}_{\mathbf{k}}$ can be systematically brought to the central cell $Y_{\mathbf{0}}$.

Writing the equation (42) for the cells $\mathbf{0}$ and $\mathbf{i}$ whose centers occupy the position $\mathbf{x_0}$ and $\mathbf{x_i}$ and making the difference for two points occupying the same position $\mathbf{y}$ respectively in the cells $\mathbf{0}$ and $\mathbf{i}$ lead to

$$\begin{aligned} B_{\mathbf{i}}(\mathbf{x_i}+\mathbf{y},\mathbf{y}) - B_{\mathbf{0}}(\mathbf{x_0}+\mathbf{y},\mathbf{y}) &= \epsilon\sigma\left(T^4_{\mathbf{i}}(\mathbf{x_i}+\mathbf{y},\mathbf{y}) - T^4_{\mathbf{0}}(\mathbf{x_0}+\mathbf{y},\mathbf{y})\right) \\ &+ (1-\epsilon)\sum_{\mathbf{k}\in\mathbb{Z}^3}\int_{\partial Y_{fs}} \mathrm{d}F_{\mathrm{d}S_{\mathbf{0}}\to\mathrm{d}S_{\mathbf{k}}}\left(B_{\mathbf{i}+\mathbf{k}} - B_{\mathbf{k}}\right) \end{aligned} \tag{44}$$

Performing a Taylor expansion of the temperature from the center $\mathbf{x_0}$ of the central cell gives:

$$T_{\mathbf{0}}(\mathbf{x_0}+\mathbf{y},\mathbf{y}) = T^{(0)}(\mathbf{x_0}) + \eta\left[\widehat{T}^{(1)} + (\mathbf{y}+\boldsymbol{\chi}(\mathbf{y}))\cdot\boldsymbol{\nabla}_x T^{(0)}\right] + \mathcal{O}(\eta^2) \tag{45}$$

We do the same development from the point $\mathbf{x}_0$ of the cell $\mathbf{0}$ to compute now the temperature in the cell $\mathbf{i}$:

$$T_{\mathbf{i}}(\mathbf{x}_0 + \boldsymbol{L}\cdot\mathbf{i}+\mathbf{y},\mathbf{y}) = T^{(0)}(\mathbf{x_0}) + \eta\left[\widehat{T}^{(1)} + (\mathbf{y}+\boldsymbol{L}\cdot\mathbf{i}+\boldsymbol{\chi}(\mathbf{y}))\cdot\boldsymbol{\nabla}_x T^{(0)}\right] + \mathcal{O}(\eta^2) \tag{46}$$

Hence for two points located at the same position $\mathbf{y}$ in the cells $\mathbf{0}$ and $\mathbf{i}$, we have:

$$T^4_{\mathbf{i}}(\mathbf{x_i}+\mathbf{y},\mathbf{y}) - T^4_{\mathbf{0}}(\mathbf{x_0}+\mathbf{y},\mathbf{y}) = 4\eta {T^{(0)}}^3\,(\boldsymbol{L}\cdot\mathbf{i})\cdot\boldsymbol{\nabla}_x T^{(0)} + \mathcal{O}(\eta^2) \tag{47}$$

As $\sum_{\mathbf{k}\in\mathbb{Z}^3}\int_{\partial Y_{fs}}\mathrm{d}F_{\mathrm{d}S_{\mathbf{0}}\to\mathrm{d}S_{\mathbf{k}}} = 1$, the solution of the previous integral equation (44) for two points occupying the same position $\mathbf{y}$ in the cells $\mathbf{0}$ and $\mathbf{i}$ satisfies

$$B_{\mathbf{i}}(\mathbf{x_i}+\mathbf{y},\mathbf{y}) - B_{\mathbf{0}}(\mathbf{x_0}+\mathbf{y},\mathbf{y}) = 4\eta\sigma {T^{(0)}}^3\,(\boldsymbol{L}\cdot\mathbf{i})\cdot\boldsymbol{\nabla}_x T^{(0)} + \mathcal{O}(\eta^2) \tag{48}$$

Equation (42) in the cell $\mathbf{0}$ now reads as

$$\begin{aligned} B^{(0)}_{\mathbf{0}} + \eta B^{(1)}_{\mathbf{0}} &= \epsilon\sigma\left(T^{(0)} + \eta T^{(1)}\right)^4 \\ &+ (1-\epsilon)\sum_{\mathbf{k}\in\mathbb{Z}^3}\int_{(\partial Y_{fs})_{\mathbf{k}}} \mathrm{d}F_{\mathrm{d}S_{\mathbf{0}}\to\mathrm{d}S_{\mathbf{k}}}\left(B^{(0)}_{\mathbf{0}} + \eta B^{(1)}_{\mathbf{0}} + 4\eta\sigma {T^{(0)}}^3(\boldsymbol{L}\cdot\mathbf{k})\cdot\boldsymbol{\nabla}_x T^{(0)}\right) \\ &+ \mathcal{O}\left(\eta^2\right) \end{aligned} \tag{49}$$

At the order $\mathcal{O}(1)$, the solution of equation (42) is $B^{(0)} = \sigma {T^{(0)}}^4(\mathbf{x})$. At the order $\mathcal{O}(\eta)$, similarly to (23), using (49) the integral equation for $B^{(1)}_{\mathbf{0}}$ is given by

$$\begin{aligned} B^{(1)}_{\mathbf{0}}(\mathbf{x},\mathbf{y}) &+ 4(1-\epsilon)\sigma {T^{(0)}}^3\mathbf{y}\cdot\boldsymbol{\nabla}_x T^{(0)} = 4\epsilon\sigma {T^{(0)}}^3\left(\widehat{T}^{(1)} + \boldsymbol{\chi}\cdot\boldsymbol{\nabla}_x T^{(0)}\right) \\ &+ (1-\epsilon)\sum_{\mathbf{k}\in\mathbb{Z}^3}\int_{\partial Y_{fs}} \mathrm{d}F_{\mathrm{d}S_{\mathbf{0}}\to\mathrm{d}S_{\mathbf{k}}}\left[B^{(1)}_{\mathbf{0}} + 4\sigma {T^{(0)}}^3\,(\boldsymbol{L}\cdot\mathbf{k}+\mathbf{y})\cdot\boldsymbol{\nabla}_x T^{(0)}\right] \end{aligned} \tag{50}$$

Note that $B_{\mathbf{0}}^{(1)}$ is function of $\mathbf{x}$ and $\mathbf{y}$. The radiosity $B_{\mathbf{0}}^{(1)}$ is sought on the $Y_{\mathbf{0}}$-cell in a form similar to (24)

$$B_{\mathbf{0}}^{(1)}(\mathbf{x},\mathbf{y}) \quad = \quad 4\sigma {T^{(0)}}^3(\mathbf{x}) \left[\widehat{T}^{(1)}(\mathbf{x}) + \boldsymbol{\beta}(\mathbf{y}) \cdot \boldsymbol{\nabla}_x T^{(0)}(\mathbf{x})\right] \tag{51}$$

where the vector $\boldsymbol{\beta}(\mathbf{y})$ with $\mathbf{y} \in (\partial Y_{fs})_{\mathbf{0}}$ is now solution of the integral equation

$$\boldsymbol{\beta} \quad = \quad \epsilon \boldsymbol{\chi} + (1-\epsilon)\left(\{\mathbf{y}+\boldsymbol{\beta}\}_F - \mathbf{y}\right) \tag{52}$$

where $\{\mathbf{y}+\boldsymbol{\beta}\}_F$ is defined by

$$\{\mathbf{y}+\boldsymbol{\beta}\}_F \quad = \quad \sum_{\mathbf{k}\in\mathbb{Z}^3} \int_{\partial Y_{fs}} \mathrm{d}F_{\mathrm{d}S_{\mathbf{0}} \to \mathrm{d}S_{\mathbf{k}}} \left(\mathbf{y}_k + \boldsymbol{\beta}_k + \boldsymbol{L}\cdot\mathbf{k}\right) \tag{53}$$

and $\mathbf{y}_k$ and $\boldsymbol{\beta}_k$ are the values of $\mathbf{y}$ and $\boldsymbol{\beta}$ in the unit cell $Y_{\mathbf{k}}$. For two opposite points located on two opposite faces of the unit cell, it can be verified that the quantity $\{\mathbf{y}+\boldsymbol{\beta}\}_F - \mathbf{y}$ is identical. Let A and B be the two opposite points on the faces $y_1 = 0$ and $y = \ell_1$ of the unit cell $Y_{\mathbf{0}}$, we have

$$\begin{aligned} \{\mathbf{y}+\boldsymbol{\beta}\}_F(\mathrm{A}) \quad &= \quad \sum_{\mathbf{k}\in\mathbb{Z}^3} \int_{\partial Y_{fs}} \mathrm{d}F_{\mathrm{d}S_{\mathrm{A}} \to \mathrm{d}S_{\mathbf{k}}} \left(\mathbf{y}_1 + \boldsymbol{\beta}_1 + \boldsymbol{L}\cdot\mathbf{k}\right) \\ \{\mathbf{y}+\boldsymbol{\beta}\}_F(\mathrm{B}) \quad &= \quad \sum_{\mathbf{k}\in\mathbb{Z}^3} \int_{\partial Y_{fs}} \mathrm{d}F_{\mathrm{d}S_{\mathrm{B}} \to \mathrm{d}S_{\mathbf{k}}} \left(\mathbf{y}_1 + \boldsymbol{\beta}_1 + \boldsymbol{L}\cdot\mathbf{k}\right) \end{aligned} \tag{54}$$

By periodicity, we have $\mathrm{d}F_{\mathrm{d}S_{\mathrm{B}} \to \mathrm{d}S_{\mathbf{k}}} = \mathrm{d}F_{\mathrm{d}S_{\mathrm{A}} \to \mathrm{d}S_{\mathbf{k}'}}$ with $\mathbf{k}' = \mathbf{k} - (1\ 0\ 0)^{\mathrm{T}}$.

$$\{\mathbf{y}+\boldsymbol{\beta}\}_F(\mathrm{B}) - \{\mathbf{y}+\boldsymbol{\beta}\}_F(\mathrm{A}) \quad = \quad \boldsymbol{L}\cdot(\mathbf{k}-\mathbf{k}') = \mathbf{y}(\mathrm{B}) - \mathbf{y}(\mathrm{A}) \tag{55}$$

As $\boldsymbol{\chi}_{f(s)}$ is a $\mathbf{y}$-periodic function, from (52) and (55), it is verified that β and $B^{(1)}$ (as $\boldsymbol{\nabla}_x T^{(0)}$ is constant) and the radiative heat flux through the gas phase are also $\mathbf{y}$-periodic.

3.2. Radiative flux

Since $\boldsymbol{\nabla}_y \cdot \mathbf{q}^{\mathrm{R}(0)} = 0$ in the fluid phase (see Section 2) according to (31), we have

$$\mathbf{q}_{\mathrm{R}}^{(0)} = \boldsymbol{\nabla}_y \cdot \left(\mathbf{q}_{\mathrm{R}}^{(0)} \otimes \mathbf{y}\right) \tag{56}$$

Averaging the preceding relation over the unit cell leads to

$$\left\langle \mathbf{q}_f^{\mathrm{R}(0)} \right\rangle \quad = \quad \frac{1}{|Y|} \int_{Y_f} \boldsymbol{\nabla}_y \cdot \left(\mathbf{q}_f^{\mathrm{R}(0)} \otimes \mathbf{y}\right) \mathrm{d}V = \frac{1}{|Y|} \int_{\partial Y_{fs} \bigcup \partial Y_{fe}} \mathbf{y} \left(\mathbf{q}_f^{\mathrm{R}(0)} \cdot \mathbf{n}_f\right) \mathrm{d}S \tag{57}$$

where ∂Y_{fe} denotes the external fluid surface of the unit cell. The first part of equation (57) on ∂Y_{fs} is calculated according to Eq. (32):

$$\frac{1}{|Y|}\int_{\partial Y_{fs}} \mathbf{y}\left(\mathbf{q}_f^{\mathrm{R}(0)}\cdot\mathbf{n}_f\right)\mathrm{d}S \;=\; -\frac{4\sigma {T^{(0)}}^3}{|Y|}\int_{\partial Y_{fs}} \mathbf{y}\otimes(\mathbf{y}+\boldsymbol{\beta}-\{\mathbf{y}+\boldsymbol{\beta}\}_F)\,\mathrm{d}S\cdot\boldsymbol{\nabla}_x T^{(0)} \quad (58)$$

The second term corresponding to the radiative exchange with neighboring cells is calculated in the frame ($\mathbf{e}_1$, $\mathbf{e}_2$, $\mathbf{e}_3$) of coordinates $\mathbf{y}$ related to the axes of the unit cell assumed to be a rectangular cuboid of sides $\ell_1\times\ell_2\times\ell_3$. Since the radiative heat flux is $\mathbf{y}$-periodic, its value is the same on two corresponding points of two parallel faces. It yields

$$\begin{aligned}\frac{1}{|Y|}\int_{\partial Y_{fe}} \mathbf{y}\left(\mathbf{q}_f^{\mathrm{R}(0)}\cdot\mathbf{n}_{fe}\right)\mathrm{d}S &= \frac{1}{|Y|}\left[\int_{y_2=0}^{\ell_2}\int_{y_3=0}^{\ell_3} q_{f1}^{\mathrm{R}(0)}\ell_1\mathbf{e}_1\mathrm{d}y_2\mathrm{d}y_3\right.\\ &\quad+\int_{y_1=0}^{\ell_1}\int_{y_3=0}^{\ell_3} q_{f2}^{\mathrm{R}(0)}\ell_2\mathbf{e}_2\mathrm{d}y_1\mathrm{d}y_3\\ &\quad\left.+\int_{y_1=0}^{\ell_1}\int_{y_2=0}^{\ell_2} q_{f3}^{\mathrm{R}(0)}\ell_3\mathbf{e}_3\mathrm{d}y_1\mathrm{d}y_2\right]\\ &= \overline{q}_{f1}^{\mathrm{R}(0)}\mathbf{e}_1+\overline{q}_{f2}^{\mathrm{R}(0)}\mathbf{e}_2+\overline{q}_{f3}^{\mathrm{R}(0)}\mathbf{e}_3 \quad (59)\end{aligned}$$

where the surface average of the radiative flux crossing the facet of normal $\mathbf{e}_1$ of the unit cell is given by

$$\begin{aligned}\overline{q}_{f1}^{\mathrm{R}(0)} &= \frac{1}{\ell_2\ell_3}\int_{y_2=0}^{\ell_2}\int_{y_3=0}^{\ell_3} q_{f1}^{\mathrm{R}(0)}\mathrm{d}y_2\mathrm{d}y_3 \quad (60)\\ &= \frac{1}{\ell_2\ell_3}\sum_{\substack{\mathbf{k}\in\mathbb{Z}^3\\ k_1<0}}\sum_{\substack{\mathbf{m}\in\mathbb{Z}^3\\ m_1\geq 0}}\int_{\partial Y_{fs}}\int_{\partial Y_{fs}}\left[4\sigma {T^{(0)}}^3(\mathbf{y}_\mathbf{k}-\mathbf{y}_\mathbf{m})\cdot\boldsymbol{\nabla}_x T^{(0)}+B_\mathbf{k}^{(1)}-B_\mathbf{m}^{(1)}\right]\gamma_1\mathrm{d}S_\mathbf{k}\mathrm{d}F_{dS_\mathbf{k}\to dS_\mathbf{m}}\end{aligned}$$

where $\gamma_1=1$ if the line joining $\mathrm{d}S_\mathbf{k}$ and $\mathrm{d}S_\mathbf{m}$ crosses the face $y_1=\ell_1$ of the central unit cell $\mathbf{0}$, 0 otherwise. Similar relationships can be written for $\overline{q}_{f2}^{\mathrm{R}(0)}$ and $\overline{q}_{f3}^{\mathrm{R}(0)}$. Since

$$B_\mathbf{k}^{(1)}-B_\mathbf{m}^{(1)}=4\sigma {T^{(0)}}^3\left[\boldsymbol{L}\cdot(\mathbf{k}-\mathbf{m})+\boldsymbol{\beta}_\mathbf{k}-\boldsymbol{\beta}_\mathbf{m}\right]\cdot\boldsymbol{\nabla}_x T^{(0)}+\mathcal{O}(\eta^2) \quad (61)$$

where $\boldsymbol{\beta}_{\mathbf{k}} = \boldsymbol{\beta}(\mathbf{y}_{\mathbf{k}})$, we have

$$\overline{q}_{f1}^{\mathrm{R}(0)} = \frac{4\sigma {T^{(0)}}^3}{\ell_2 \ell_3} \times \sum_{\substack{\mathbf{k} \in \mathbb{Z}^3 \\ k_1 < 0}} \sum_{\substack{\mathbf{m} \in \mathbb{Z}^3 \\ m_1 \geq 0}} \left[\int_{\partial Y_{fs}} \int_{\partial Y_{fs}} \left[\boldsymbol{L} \cdot (\mathbf{k} - \mathbf{m}) + \mathbf{y}_k + \boldsymbol{\beta}_{\mathbf{k}} - \mathbf{y}_{\mathbf{m}} - \boldsymbol{\beta}_{\mathbf{m}} \right] \gamma_1 \mathrm{d}S_{\mathbf{0}} \, \mathrm{d}F_{\mathrm{d}S_{\mathbf{0}} \to \mathrm{d}S_{\mathbf{m}-\mathbf{k}}} \right] \cdot \boldsymbol{\nabla}_x T^{(0)}$$

$$= -4\sigma {T^{(0)}}^3 \boldsymbol{\alpha}^1 \cdot \boldsymbol{\nabla}_x T^{(0)} \quad (62)$$

Here, $\boldsymbol{\alpha}^1$ is a vector whose coordinates are a length. Finally, the average radiative flux reads as

$$\left\langle \mathbf{q}_f^{\mathrm{R}(0)} \right\rangle = -4\sigma {T^{(0)}}^3 \left(\frac{1}{|Y|} \int_{\partial Y_{fs}} \mathbf{y} \otimes (\mathbf{y} + \boldsymbol{\beta} - \{\mathbf{y} + \boldsymbol{\beta}\}_F) \, \mathrm{d}S + \boldsymbol{\alpha} \right) \cdot \boldsymbol{\nabla}_x T^{(0)} = -\boldsymbol{\lambda}^{\mathrm{R}} \cdot \boldsymbol{\nabla}_x T^{(0)} \quad (63)$$

where $\boldsymbol{\alpha} = \left[\boldsymbol{\alpha}^1 \quad \boldsymbol{\alpha}^2 \quad \boldsymbol{\alpha}^3 \right]^{\mathrm{T}}$ is a square matrix. Since the radiative incoming flux into the cell $Y_{\mathbf{0}}$ is the same as the outgoing flux for two points of the external surface of the cell corresponding to each other by periodicity and as $\boldsymbol{\nabla}_y \cdot \mathbf{q}^{\mathrm{R}(0)} = 0$, the global radiative contribution on the fluid-solid interface is zero. The problem (27) for $\boldsymbol{\chi}$ satisfies thus the necessary existence condition. As discussed in Section 2, the effective conductivity of the homogenized medium is obtained as

$$\boldsymbol{\lambda}_{eq} = n_f \lambda_f \left(\boldsymbol{I} + \langle \boldsymbol{\nabla}_y \boldsymbol{\chi}_f \rangle^f \right) + \boldsymbol{\lambda}^{\mathrm{R}} + n_s \lambda_s \left(\boldsymbol{I} + \langle \boldsymbol{\nabla}_y \boldsymbol{\chi}_s \rangle^s \right) \quad (64)$$

which depends on the radiation through the term $\boldsymbol{\lambda}^{\mathrm{R}}$. This is an important result highlighting that the radiation at the macroscopic scale only modifies the apparent conductivity.

4. Homogenization for the convection-diffusion-radiation problem

In this section, we now consider heat transfer by convection through the fluid phase together with the diffusion-radiation problem. In this context, a new non-dimensional number appears, the Péclet number $\mathrm{Pe} = v_f^{ref} L / a_f$ where v_f^{ref} is the average velocity chosen as a reference. The order of magnitude of the Péclet number depends obviously on the fluid velocity. The most interesting case is $\mathrm{Pe} = \mathcal{O}(\eta^{-1})$ which corresponds to the so-called Taylor dispersion regime containing all the results for lower orders of magnitude of the Péclet number. For higher orders of magnitude of the Péclet number, it has been well discussed in [35] that this case leads to a so-called non-homogenizable situation. In the Taylor regime, the microscopic convective time in the fluid phase

(ℓ/v_f^{ref}) is of the same magnitude as the diffusion time ℓ^2/a_f. The physical properties of the fluid and the solid phases are assumed to be of the same order of magnitude.

Two methods are available to homogenize this dispersion problem: first the method introduced by Auriault and Adler [35] and used by Moyne et al. [33] to study thermal dispersion and secondly the drift method introduced by Allaire et al. [38]. Both methods lead to almost the same result and the second method will be considered here.

4.1. Problem to be solved

The problem is first written in a non-dimensional form. Two macroscopic time scales exist: diffusive and convective ones corresponding to L^2/a_f and L/v_f^{ref} respectively. The diffusive time is chosen as the reference time and this choice will be explained further. The conductive flux and radiative fluxes are assumed to be of the same order of magnitude at the macroscale. The problem to be solved can be written in dimensional form with powers of η formally indicating the order of magnitude of each term.

$$\left\{\begin{array}{rcll} (\rho c)_f\left[\dfrac{\partial T_f}{\partial t}+\dfrac{\mathbf{v}_f}{\eta}\cdot\boldsymbol{\nabla}T_f\right] &=& \boldsymbol{\nabla}\cdot\left(\lambda_f\boldsymbol{\nabla}T_f-\mathbf{q}^{\mathrm{R}}\right) & \text{in } Y_f \\ (\rho c)_s\dfrac{\partial T_s}{\partial t} &=& \boldsymbol{\nabla}\cdot\left(\lambda_s\boldsymbol{\nabla}T_s\right) & \text{in } Y_s \\ T_f &=& T_s & \\ -\lambda_f\boldsymbol{\nabla}T_f\cdot\mathbf{n}_f-\lambda_s\boldsymbol{\nabla}T_s\cdot\mathbf{n}_s &=& \mathbf{q}^{\mathrm{R}}\cdot\mathbf{n}_f=\dfrac{1}{\eta}\left(B-\{B\}_F\right) & \text{on } \partial Y_{fs} \end{array}\right. \tag{65}$$

$$\text{with}\quad \boldsymbol{\nabla}=\boldsymbol{\nabla}_x+\frac{1}{\eta}\boldsymbol{\nabla}_y$$

where B is solution of the integral equation (42).

4.2. Problem for $T^{(0)}$

The problem in $T^{(0)}$ at the order $\mathcal{O}(\eta^{-2})$ in Y_s is written:

$$\left\{\begin{array}{rcll} (\rho c)_f\mathbf{v}_f\cdot\boldsymbol{\nabla}_y T_f^{(0)} &=& \boldsymbol{\nabla}_y\cdot\left(\lambda_f\boldsymbol{\nabla}_y T_f^{(0)}-\mathbf{q}^{\mathrm{R}(-1)}\right) & \text{in } Y_f \\ 0 &=& \boldsymbol{\nabla}_y\cdot\left(\lambda_s\boldsymbol{\nabla}_y T_s^{(0)}\right) & \text{in } Y_s \\ T_f^{(0)} &=& T_s^{(0)} & \\ -\lambda_f\boldsymbol{\nabla}_y T_f^{(0)}\cdot\mathbf{n}_f-\lambda_s\boldsymbol{\nabla}_y T_s^{(0)}\cdot\mathbf{n}_s &=& -\mathbf{q}^{\mathrm{R}(-1)}\cdot\mathbf{n}_f=B^{(0)}-\{B^{(0)}\}_F & \text{on } \partial Y_{fs} \end{array}\right. \tag{66}$$

whose solution is $T_f^{(0)}(t,\mathbf{x},\mathbf{y})=T_s^{(0)}(t,\mathbf{x},\mathbf{y})\equiv T^{(0)}(t,\mathbf{x})$, $B^{(0)}=\left\{B^{(0)}\right\}_F=\sigma {T^{(0)}}^4$ and $\mathbf{q}^{\mathrm{R}(-1)}\equiv 0$.

4.3. Problem for $T^{(1)}$

The integral equation for $B^{(1)}$ is identical to equation (50) whose solution is given by (51) where the vector $\boldsymbol{\beta}$ is solution of the integral equation (52).

The problem for $T^1_{f(s)}$ is written in a frame moving at a *drift* velocity $\widetilde{\mathbf{v}}$ (to be determined further) of the same order of magnitude as the flow velocity v_f^{ref}. In the moving frame, the convective heat motion is "cancelled" and the reference time is the macroscopic diffusive time L^2/a_f. Thus $\widetilde{\mathbf{x}} = \mathbf{x} - \widetilde{\mathbf{v}}t/\epsilon$ and $T^1_{f(s)}$ is searched in the form $T^1_{f(s)}(\widetilde{\mathbf{x}}, \mathbf{y})$. The derivation operators are defined as

$$\left.\frac{\partial}{\partial t}\right|_x = \left.\frac{\partial}{\partial t}\right|_{\widetilde{x}} - \frac{\widetilde{\mathbf{v}}}{\epsilon}\cdot\boldsymbol{\nabla}_x \tag{67}$$

$$\boldsymbol{\nabla} = \boldsymbol{\nabla}_{\widetilde{x}} + \frac{1}{\epsilon}\boldsymbol{\nabla}_y \qquad (\boldsymbol{\nabla}_x = \boldsymbol{\nabla}_{\widetilde{x}}) \tag{68}$$

The problem is written as

$$\left\{\begin{array}{rcll} (\rho c)_f\left[-\widetilde{\mathbf{v}}\cdot\boldsymbol{\nabla}_x T^{(0)} + \mathbf{v}_f\cdot\left(\boldsymbol{\nabla}_y T_f^{(1)} + \boldsymbol{\nabla}_x T^{(0)}\right)\right] &=& \boldsymbol{\nabla}_y\cdot\left(\lambda_f\boldsymbol{\nabla}_y T_f^{(1)}\right) - \boldsymbol{\nabla}_y\cdot\mathbf{q}^{\mathrm{R}(0)} & \text{in } Y_f \\ -(\rho c)_s\widetilde{\mathbf{v}}\cdot\boldsymbol{\nabla}_x T^0 &=& \boldsymbol{\nabla}_y\cdot\left(\lambda_s\boldsymbol{\nabla}_y T_s^{(1)}\right) & \text{in } Y_s \end{array}\right. \tag{69}$$

with the following transmission conditions on the interface ∂Y_{fs}

$$\left\{\begin{array}{rcl} T_f^{(1)} &=& T_s^{(1)} \\ -\lambda_f\left(\boldsymbol{\nabla}_y T_f^{(1)} + \boldsymbol{\nabla}_x T^{(0)}\right)\cdot\mathbf{n}_f & & \\ -\lambda_s\left(\boldsymbol{\nabla}_y T_s^{(1)} + \boldsymbol{\nabla}_x T^{(0)}\right)\cdot\mathbf{n}_s &=& -\mathbf{q}^{\mathrm{R}(0)}\cdot\mathbf{n}_f \end{array}\right. \tag{70}$$

with $\mathbf{q}^{R(0)}$ given by Equation (26). The solution is searched in the form

$$T^{(1)}_{f(s)}(t,\widetilde{\mathbf{x}},\mathbf{y}) = \widehat{T}^{(1)}(t,\widetilde{\mathbf{x}}) + \boldsymbol{\chi}_{f(s)}(\mathbf{y})\cdot\boldsymbol{\nabla}_x T^{(0)}(t,\widetilde{\mathbf{x}}) \tag{71}$$

$$B^{(1)}(t,\widetilde{\mathbf{x}},\mathbf{y}) = 4\sigma {T^{(0)}}^3(t,\widetilde{\mathbf{x}})\left[\widehat{T}^{(1)}(t,\widetilde{\mathbf{x}}) + \boldsymbol{\beta}(\mathbf{y})\cdot\boldsymbol{\nabla}_x T^{(0)}(t,\widetilde{\mathbf{x}})\right] \tag{72}$$

where $\widehat{T}^{(1)}(\widetilde{\mathbf{x}},t)$ plays the role of an integration constant and $\boldsymbol{\chi}_{f(s)}(\mathbf{y})$ is solution of

$$\left\{\begin{array}{rcll} (\rho c)_f\left(-\widetilde{\mathbf{v}} + \mathbf{v}_f + \mathbf{v}_f\cdot\boldsymbol{\nabla}_y\boldsymbol{\chi}_f\right) &=& \boldsymbol{\nabla}_y\cdot\left(\lambda_f\boldsymbol{\nabla}_y\boldsymbol{\chi}_f\right) & \text{in } Y_f \\ 0 &=& \boldsymbol{\nabla}_y\cdot\mathbf{q}^{\mathrm{R}(0)} & \\ -(\rho c)_s\widetilde{\mathbf{v}} &=& \boldsymbol{\nabla}_y\cdot\left(\lambda_s\boldsymbol{\nabla}_y\boldsymbol{\chi}_s\right) & \text{in } Y_s \\ \boldsymbol{\chi}_f &=& \boldsymbol{\chi}_s & \\ -\mathbf{n}_f\cdot\lambda_f\left(\boldsymbol{I} + \boldsymbol{\nabla}_y\boldsymbol{\chi}_f\right) & & & \\ -\mathbf{n}_s\cdot\lambda_s\left(\boldsymbol{I} + \boldsymbol{\nabla}_y\boldsymbol{\chi}_s\right) &=& 4\epsilon\sigma {T^{(0)}}^3\left(\mathbf{y} + \boldsymbol{\beta} - \{\mathbf{y}+\boldsymbol{\beta}\}_F\right) & \text{on } \partial Y_{fs} \end{array}\right. \tag{73}$$

where the vector $\boldsymbol{\beta}$ is solution of the integral vector equation (52).

The necessary and sufficient condition for the previous problem to have a solution is that the sum of the sources is zero. On the interfaces ∂Y_{fs}, the sum of the conductive and radiative sources is null. Therefore, it is necessary that the volume average of the convective source terms is null:

$$n_f(\rho c)_f \left(-\widetilde{\mathbf{v}} + \langle \mathbf{v}_f \rangle^f\right) - n_s(\rho c)_s \widetilde{\mathbf{v}} = 0 \quad \text{or} \quad \widetilde{\mathbf{v}} = \frac{n_f(\rho c)_f}{\langle \rho c \rangle} \langle \mathbf{v}_f \rangle^f = \gamma_f \langle \mathbf{v}_f \rangle^f \tag{74}$$

with $\langle \rho c \rangle = n_f(\rho c)_f + n_s(\rho c)_s$ and $\gamma_{f(s)} = n_{f(s)}(\rho c)_{f(s)} / \langle \rho c \rangle$, $\gamma_f + \gamma_s = 1$.

The problem for $\boldsymbol{\chi}_{f(s)}$ is finally written:

$$\left\{ \begin{array}{rcll} (\rho c)_f \left(\mathbf{v}_f - \gamma_f \langle \mathbf{v}_f \rangle^f + \mathbf{v}_f \cdot \boldsymbol{\nabla}_y \boldsymbol{\chi}_f\right) & = & \boldsymbol{\nabla}_y \cdot \left(\lambda_f \boldsymbol{\nabla}_y \boldsymbol{\chi}_f\right) & \text{in } Y_f \\ -(\rho c)_s \gamma_f \langle \mathbf{v}_f \rangle^f & = & \boldsymbol{\nabla}_y \cdot \left(\lambda_s \boldsymbol{\nabla}_y \boldsymbol{\chi}_s\right) & \text{in } Y_s \\ \boldsymbol{\chi}_f & = & \boldsymbol{\chi}_s & \\ -\mathbf{n}_f \cdot \lambda_f \left(\boldsymbol{I} + \boldsymbol{\nabla}_y \boldsymbol{\chi}_f\right) & & & \\ -\mathbf{n}_s \cdot \lambda_s \left(\boldsymbol{I} + \boldsymbol{\nabla}_y \boldsymbol{\chi}_s\right) & = & 4\epsilon\sigma {T^{(0)}}^3 \left(\mathbf{y} + \boldsymbol{\beta} - \{\mathbf{y} + \boldsymbol{\beta}\}_F\right) & \text{on } \partial Y_{fs} \end{array} \right. \tag{75}$$

Note that the problems for $T^{(1)}$ and $\boldsymbol{\chi}$ are defined to within one additive constant. For the uniqueness of the solution, we impose

$$n_f(\rho c)_f \left\langle \boldsymbol{\chi}_f \right\rangle^f + n_s(\rho c)_s \left\langle \boldsymbol{\chi}_s \right\rangle^s = 0 \tag{76}$$

which leads to

$$\widehat{T}^{(1)}(\mathbf{x}, t) = n_f(\rho c)_f \langle T_f^{(1)} \rangle^f + n_s(\rho c)_s \left\langle T_s^{(1)} \right\rangle^s \equiv \langle T^{(1)} \rangle \tag{77}$$

where $\left\langle T^{(1)} \right\rangle$ is the enthalpic average temperature of the medium at the order $\mathcal{O}(\eta)$.

4.4. Problem for $T^{(2)}$

The problem for $T^{(2)}$ at the order $\mathcal{O}(\eta^0)$ is written as

$$\left\{ \begin{array}{l} (\rho c)_f \left[\left. \dfrac{\partial T^{(0)}}{\partial t} \right|_{\widetilde{x}} - \widetilde{\mathbf{v}} \cdot \boldsymbol{\nabla}_x T_f^{(1)} + \mathbf{v}_f \cdot \left(\boldsymbol{\nabla}_x T^{(1)} + \boldsymbol{\nabla}_y T_f^{(2)}\right) \right] = \\ \boldsymbol{\nabla}_y \cdot \left[\lambda_f \left(\boldsymbol{\nabla}_x T_f^{(1)} + \boldsymbol{\nabla}_y T_f^{(2)}\right) - \mathbf{q}_R^{(1)}\right] + \boldsymbol{\nabla}_x \cdot \left[\lambda_f \left(\boldsymbol{\nabla}_x T^{(0)} + \boldsymbol{\nabla}_y T_f^{(1)}\right) - \mathbf{q}_R^{(0)}\right] \quad \text{in } Y_f \\ (\rho c)_s \left[\left. \dfrac{\partial T^{(0)}}{\partial t} \right|_{\widetilde{x}} - \widetilde{\mathbf{v}} \cdot \boldsymbol{\nabla}_x T_s^{(1)} \right] = \\ \boldsymbol{\nabla}_y \cdot \left[\lambda_s \left(\boldsymbol{\nabla}_x T_s^{(1)} + \boldsymbol{\nabla}_y T_s^{(2)}\right)\right] + \boldsymbol{\nabla}_x \cdot \left[\lambda_s \left(\boldsymbol{\nabla}_x T^{(0)} + \boldsymbol{\nabla}_y T_s^{(1)}\right)\right] \quad \text{in } Y_s \\ T_f^{(2)} = T_s^{(2)} \quad \text{on } \partial Y_{fs} \\ -\lambda_f \left(\boldsymbol{\nabla}_x T_f^{(1)} + \boldsymbol{\nabla}_y T_f^{(2)}\right) \cdot \mathbf{n}_f - \lambda_s \left(\boldsymbol{\nabla}_x T_s^{(1)} + \boldsymbol{\nabla}_y T_s^{(2)}\right) \cdot \mathbf{n}_s = -\mathbf{q}^{R(1)} \cdot \mathbf{n}_f \end{array} \right. \tag{78}$$

The compatibility condition is obtained by integrating the preceding equation over the volume of the unit cell. Note that using the divergence theorem

$$\left\langle \mathbf{v}_f \cdot \boldsymbol{\nabla}_y T_f^{(2)} \right\rangle^f = \left\langle \boldsymbol{\nabla}_y \cdot \left(T_f^{(2)} \mathbf{v}_f \right) \right\rangle^f = 0 \tag{79}$$

as the velocity is null on the fluid-solid interface ∂Y_{fs} and due to periodicity conditions on the fluid frontiers of the unit-cell ∂Y_{fe}. Moreover

$$\left\langle \boldsymbol{\nabla}_x T_f^{(1)} \right\rangle^f = \boldsymbol{\nabla}_x \left\langle T_f^{(1)} \right\rangle^f = \boldsymbol{\nabla}_x \left(\left\langle \boldsymbol{\chi}_f \right\rangle^f \cdot \boldsymbol{\nabla}_x T^{(0)} + \left\langle T^{(1)} \right\rangle \right) \tag{80}$$

Thanks to the periodicity of the radiative flux, the integral of the terms in $\boldsymbol{\nabla}_y$ also vanishes

$$\begin{aligned} \int_{Y_f} \boldsymbol{\nabla}_y \cdot \left[\lambda_f \left(\boldsymbol{\nabla}_x T_f^{(1)} + \boldsymbol{\nabla}_y T_f^{(2)} \right) \right] \mathrm{d}V + \int_{Y_s} \boldsymbol{\nabla}_y \cdot \left[\lambda_s \left(\boldsymbol{\nabla}_x T_s^{(1)} + \boldsymbol{\nabla}_y T_s^{(2)} \right) \right] \mathrm{d}V = \\ \int_{\partial Y_{fs} + \partial Y_{fe}} \lambda_f \left(\boldsymbol{\nabla}_x T_f^{(1)} + \boldsymbol{\nabla}_y T_f^{(2)} \right) \cdot \mathbf{n}_f \mathrm{d}S + \int_{\partial Y_{fs} + \partial Y_{se}} \lambda_s \left(\boldsymbol{\nabla}_x T^{(1)} + \boldsymbol{\nabla}_y T_s^{(2)} \right) \cdot \mathbf{n}_s \mathrm{d}S = \\ \int_{\partial Y_{fs}} \mathbf{q}^{R(1)} \cdot \mathbf{n}_f \mathrm{d}S = 0 \end{aligned} \tag{81}$$

The surface integrals cancel each other by periodicity on the external borders of the cell ∂Y_{fe} and ∂Y_{se}. On ∂Y_{fs}, the condition on the normal flux at the interface (78c) is used. For the radiative term, the null value of the integral on ∂Y_{fs} comes from the divergence-free property of the radiative flux and from its periodicity on the cell frontier. Finally, the result is written

$$\begin{aligned} \langle \rho c \rangle \left. \frac{\partial T^{(0)}}{\partial t} \right|_{\widetilde{x}} - n_f (\rho c)_f \widetilde{\mathbf{v}} \cdot \boldsymbol{\nabla}_x \left(\left\langle \boldsymbol{\chi}_f \right\rangle^f \cdot \boldsymbol{\nabla}_x T^{(0)} + \left\langle T^{(1)} \right\rangle \right) \\ + n_f (\rho c)_f \left\langle \mathbf{v}_f \cdot \boldsymbol{\nabla}_x \left(\boldsymbol{\chi}_f \cdot \boldsymbol{\nabla}_x T^{(0)} + \left\langle T^{(1)} \right\rangle \right) \right\rangle^f - n_s (\rho c)_s \widetilde{\mathbf{v}} \cdot \boldsymbol{\nabla}_x \left(\left\langle \boldsymbol{\chi}_s \right\rangle^s \cdot \boldsymbol{\nabla}_x T^{(0)} + \left\langle T^{(1)} \right\rangle \right) \\ = \boldsymbol{\nabla}_x \cdot \left\{ \left[n_f \lambda_f \left(\boldsymbol{I} + \left\langle \boldsymbol{\nabla}_y \boldsymbol{\chi}_f \right\rangle^f \right) + \boldsymbol{\lambda}^{\mathrm{R}} + n_s \lambda_s \left(\boldsymbol{I} + \left\langle \boldsymbol{\nabla}_y \boldsymbol{\chi}_s \right\rangle^s \right) \right] \cdot \boldsymbol{\nabla}_x T^{(0)} \right\} \end{aligned} \tag{82}$$

where $\boldsymbol{\lambda}^{\mathrm{R}}$ is defined by equation (63). Taking into account relation (76) yields

$$\langle \rho c \rangle \left(\left. \frac{\partial T^{(0)}}{\partial t} \right|_{\widetilde{\mathbf{x}}} - \widetilde{\mathbf{v}} \cdot \boldsymbol{\nabla}_x \left\langle T^{(1)} \right\rangle \right) + n_f (\rho c)_f \left\langle \mathbf{v}_f \right\rangle^f \cdot \boldsymbol{\nabla}_x \left\langle T^{(1)} \right\rangle = \boldsymbol{\nabla}_x \cdot \left(\boldsymbol{\Lambda}_{disp} \cdot \boldsymbol{\nabla}_x T^{(0)} \right) \tag{83}$$

with

$$\boldsymbol{\Lambda}_{disp} = n_f \lambda_f \left(\boldsymbol{I} + \left\langle \boldsymbol{\nabla}_y \boldsymbol{\chi}_f \right\rangle^f \right) + \boldsymbol{\lambda}^{\mathrm{R}} + n_s \lambda_s \left(\boldsymbol{I} + \left\langle \boldsymbol{\nabla}_y \boldsymbol{\chi}_s \right\rangle^s \right) - n_f (\rho c)_f \left\langle \mathbf{v}_f \boldsymbol{\chi}_f \right\rangle^f \tag{84}$$

Coming back to the fixed frame of the laboratory at the order $\mathcal{O}\left(\eta^0\right)$, we have:

$$\langle \rho c \rangle \left. \frac{\partial \langle T \rangle}{\partial t} \right|_x + n_f (\rho c)_f \left\langle \mathbf{v}_f \right\rangle^f \cdot \boldsymbol{\nabla}_x \langle T \rangle = \boldsymbol{\nabla}_x \cdot \left(\boldsymbol{\Lambda}_{disp} \cdot \boldsymbol{\nabla}_x \langle T \rangle \right) \tag{85}$$

where $\langle T \rangle = T^{(0)} + \langle T^{(1)} \rangle \simeq T^{(0)}$ adding the terms $\left. \frac{\partial \langle T^{(1)} \rangle}{\partial t} \right|_{\widetilde{x}}$ and $\boldsymbol{\nabla}_x \cdot \left(\boldsymbol{\Lambda}_{disp} \cdot \boldsymbol{\nabla}_x \langle T^{(1)} \rangle \right)$, which have the order of magnitude $\mathcal{O}(\eta)$. The consideration of radiative transfer for the convection-diffusion transport in porous media only modifies the diffusion-dispersion tensor.

It should be noted that the equivalent conductivity tensor (84) can be straightforwardly reduced to the conduction-dispersion coefficient reported in [33] in the case without radiation effect.

5. Numerical simulations and validation of the model

The aim of this section is to derive an analytical solution of the effective conductivity (84) in the case of a porous medium made of an arrangement of circular cylindrical parallel pores. This solution will be compared with direct numerical simulations of the microscopic model in order to validate the macroscopic model.

5.1. Analytical solution

To derive an analytical solution, instead of considering a cubic unit cell, the problem is reduced to periodic unit cells composed of a thin layer of an outer cylinder of radius r_1 made of a solid phase of thermal conductivity λ_s together with an inner cylinder of radius r_0 occupied by a fluid phase of conductivity λ_f (see Figure 1). It should be emphasized that the problem in the unit cell is independent on the longitudinal axis of the cylinder. The periodicity conditions refer to the equality of the (vector) functions and their normal derivative at two diametrically opposite points on the outer boundary of the domain as described in Chang [39].

Due to the cell geometry (a disk), the vectors $\boldsymbol{\beta}$ and $\boldsymbol{\chi}$ do not depend on y_1 and are therefore given by

$$\boldsymbol{\beta} = \beta_1 \, \widehat{\mathbf{e}}_1 + \beta_r \, \widehat{\mathbf{e}}_r \tag{86}$$

$$\boldsymbol{\chi} = \chi_1(r) \, \widehat{\mathbf{e}}_1 + \chi_r(r) \, \widehat{\mathbf{e}}_r \tag{87}$$

where $\widehat{\mathbf{e}}_1$ is the unit vector parallel to the axis of the cylinder, $\widehat{\mathbf{e}}_r = \mathbf{r}/r$ the radial vector. β_1 and β_r are constant. χ_1 and χ_r are functions of r.

The calculations of $\boldsymbol{\beta}$, χ and $\boldsymbol{\alpha}$ in this geometry are detailed in Appendix B. The main result obtained for the effective conductivity are given as follows.

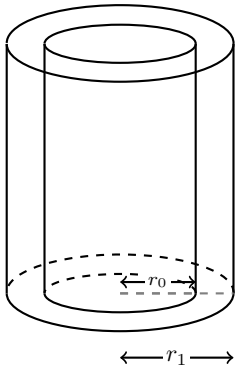

Figure 1: Fluid flow through a cylinder

The macroscopic equation for $\langle T \rangle$ is given by:

$$\langle \rho c \rangle \frac{\partial \langle T \rangle}{\partial t} + n_f \langle v_f \rangle^f \frac{\partial \langle T \rangle}{\partial x_1} = \boldsymbol{\nabla} \cdot (\boldsymbol{\Lambda}_{disp} \cdot \boldsymbol{\nabla} \langle T \rangle) \tag{88}$$

with the effective conductivity $\boldsymbol{\Lambda}_{disp}$ is composed of dispersion and radiation parts $\boldsymbol{\lambda}^D$ and $\boldsymbol{\lambda}^{\mathrm{R}}$ respectively:

$$\boldsymbol{\Lambda}_{disp} \quad = \quad \boldsymbol{\lambda}^D + \boldsymbol{\lambda}^{\mathrm{R}} \tag{89}$$

The dispersion tensor is given by:

$$\begin{aligned} \boldsymbol{\lambda}^{\mathrm{D}} \quad &= \quad \Big\{ n_f \lambda_f + n_s \lambda_s \\ &+ \quad n_f \lambda_f \mathrm{Pe}^2 \left[\frac{6\gamma_f^2 - 16\gamma_f + 11}{48} - \frac{a_f (\rho c)_f (\rho c)_s (2 \log n_f - 4 n_f + n_f^2 + 3)}{8 a_s \langle \rho c \rangle^2} \right] \Big\} \widehat{\mathbf{e}}_1 \otimes \widehat{\mathbf{e}}_1 \end{aligned} \tag{90}$$

$$\tag{91}$$

with the Péclet number is defined as $\mathrm{Pe} = \dfrac{\langle v_f \rangle^f r_0}{a_f}$.

The radiative tensor is given by:

$$\boldsymbol{\lambda}^{\mathrm{R}} \quad = \quad \begin{pmatrix} \dfrac{32 n_f \epsilon \sigma {T^{(0)}}^3 r_0}{3} & 0 & 0 \\ 0 & \lambda_{2\mathrm{D}}^{eff} & 0 \\ 0 & 0 & \lambda_{2\mathrm{D}}^{eff} \end{pmatrix} \tag{92}$$

where $\boldsymbol{\lambda}_{11}^{\mathrm{R}}$ is the effective radiation conductivity in the longitudinal direction whereas $\boldsymbol{\lambda}_{22}^{\mathrm{R}} = \boldsymbol{\lambda}_{33}^{\mathrm{R}} = \lambda_{2\mathrm{D}}^{eff}$ represents the effective radiation conductivity in the radial direction given by:

$$\lambda_{\mathrm{2D}}^{eff} = \lambda_s \frac{(1+n_f)\lambda_f^* + (1-n_f)\lambda_s}{(1-n_f)\lambda_f^* + (1+n_f)\lambda_s} \tag{93}$$

with

$$\lambda_f^* = \lambda_f + \frac{16\epsilon\sigma {T^{(0)}}^3 r_0}{4-\epsilon} \tag{94}$$

5.2. Numerical results

Direct numerical simulations are carried out in order to compare with the macroscopic results (88-94) for a cylindrical geometry.

First, the longitudinal effective dispersion-radiation coefficient result (92) is used to solve the macroscopic equation (88) in one dimension. The parameters used in simulations are presented in Table. 1. At the inlet $z = 0$, a fluid flux of velocity v_f and temperature T_{in} enters the porous medium initially at temperature T_{ini}. At the outlet $z = L_z$, Danckwerts condition (closed to conduction) is imposed. Moreover, a Poiseuille flow in a cylindrical pore is considered for the fluid phase. On the other hand, direct numerical simulations (DNS) resolve the unsteady pore-scale model in three dimensions using COMSOL Multyphysics 5.6 with similar conditions to the macroscopic simulation. In Figure 2(a), the averaged temperature of the fluid phase at the middle point $z = L_z/2$ is plotted versus time. The results obtained by DNS and predicted by the macroscopic law are in very good agreement with a relative error around 2% represented in Figure 2(b). This comparison proves the accuracy of the homogenized result in the longitudinal direction.

Secondly, the homogenized result in radial direction (B.32) is verified by comparison with DNS. The unit cell of the porous medium of porosity n_f is made of a cylindrical pore of diameter r_0 in a solid cube. For the DNS on the lower and upper faces, Dirichlet conditions with two fixed temperatures T_c and T_f ($T_c > T_f$) are imposed whereas periodicity conditions are considered for the other ones (see Figure 3). In this configuration, the effective conductivity λ_{2D}^{eff} can be estimated from the averaged flux on the two faces and the temperature difference $T_c - T_f$. In Figure 4(a), the effective conductivity in the radial direction given by the DNS and the homogenized result are displayed according to the averaged medium temperature of the medium. Excellent agreement between both approaches is observed with a relative error of around 2% (see Figure 4(b)). The effective coefficient increases with the averaged temperature when the radiation contribution

Parameter	Symbol	Value	Unit
Pore Radius	r_0	2	mm
Porosity	n_f	0.5	-
Cylinder length	L_z	100	mm
Fluid thermal conductivity	λ_f	0.03	$\mathrm{W.m^{-1}.K^{-1}}$
Solid thermal conductivity	λ_s	1	$\mathrm{W.m^{-1}.K^{-1}}$
Fluid density	ρ_f	1	$\mathrm{kg.m^{-3}}$
Solid density	ρ_s	1000	$\mathrm{kg.m^{-3}}$
Fluid heat capacity	c_f	1000	$\mathrm{J.kg^{-1}.K^{-1}}$
Solid heat capacity	c_s	1000	$\mathrm{J.kg^{-1}.K^{-1}}$
Averaged fluid velocity	v_f	0.1	$\mathrm{m.s^{-1}}$
Initial temperature	T_{ini}	1000	K
Inlet temperature	T_{in}	990	K

Table 1: Parameters used in the simulation

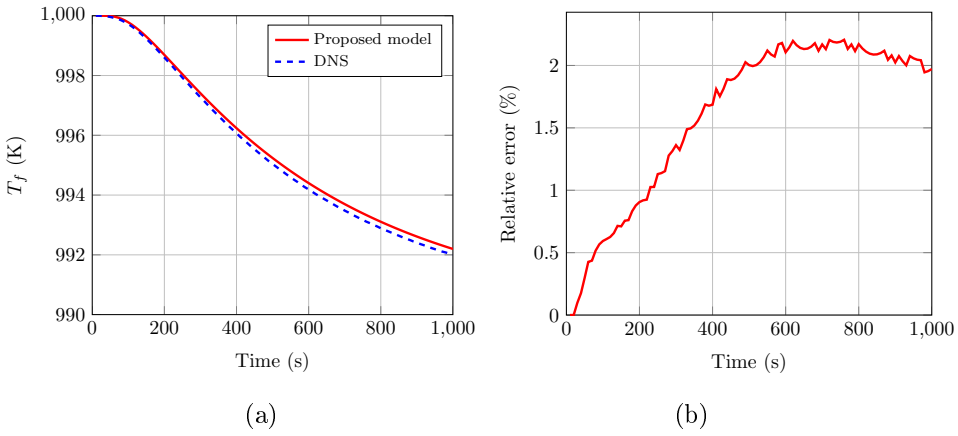

Figure 2: (a) Temperature of the fluid phase at $z = Lz/2$ vs time obtained from the proposed model and the DNS (b) Relative error.

increases as expected. Again, the upscaling approach provides a very accurate approximation to estimate the macroscopîc effective coefficients.

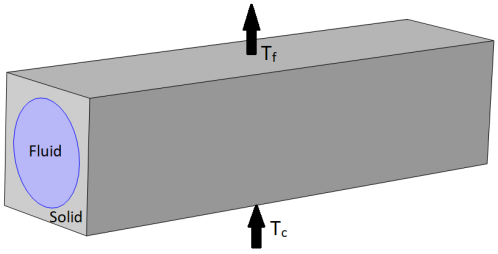

Figure 3: 3D domain for the DNS to compute the effective conductivity in radial direction.

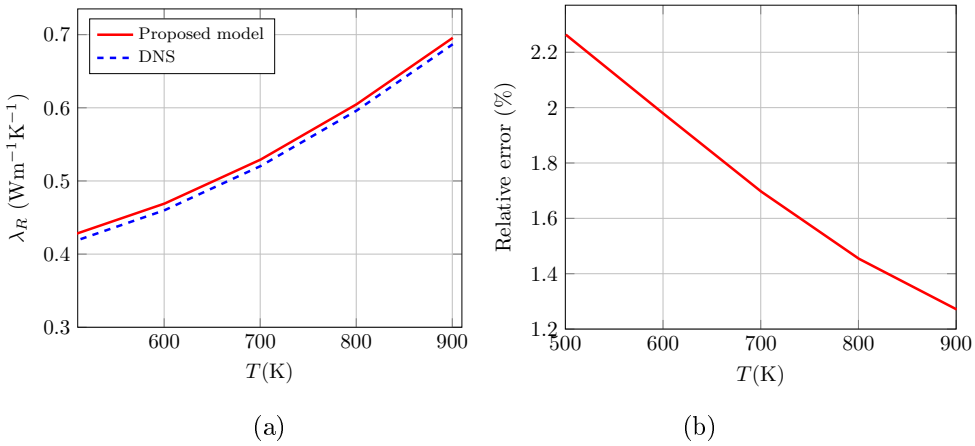

Figure 4: (a) Effective conductivity in radial direction vs temperature obtained from the proposed model and the DNS (b) Relative error.

6. Conclusion

A multiscale approach based on the homogenization technique has been developed to study the conduction-convection-radiation coupled problem in porous media. The surface-to-surface radiation is investigated for both closed and connected-pores systems. The latter is combined with the convection problem in the fluid phase. Macroscopic results obtained from the periodic homogenization procedure highlight that radiation modifies the effective conduction coefficient of the macroscopic one temperature-equation through a radiative term λ^R. In addition, the classical closure problem for the conductive part is also modified by the local surface-to-surface radiation. Application to a specific geometry of cylindrical pores allows to analytically derive the effective coefficients issued from the homogenization results. Direct numerical simulations of the pore-scale model carried out

with COMSOL Multiphysics show an excellent agreement with the numerical results obtained from the homogenized models. This underlines the accuracy of the proposed approach for estimating the effective coefficients.

This work contributes to a better understanding of the form of the macroscopic equation to be used to describe a conduction-convection-radiation transport problem in porous media. Although the closure problems are difficult to be numerically solved in complex geometries, the form of the macroscopic laws is rigorously derived by a periodic homogenization technique. This form can be used to identify the model parameters in real or numerical experiments.

Appendix A. Application to particular geometries

Appendix A.1. Parallel layers

The proposed model is now applied to the case of a medium consisting of periodic parallel solid layers of thickness $2e_s$ and fluid layers of thickness $2e_f$ (see Figure A.5). Consider the unit cell located at $-(e_s + e_f) < y_1 < e_s + e_f$. It is a closed-inclusion problem for a monodimensional medium.

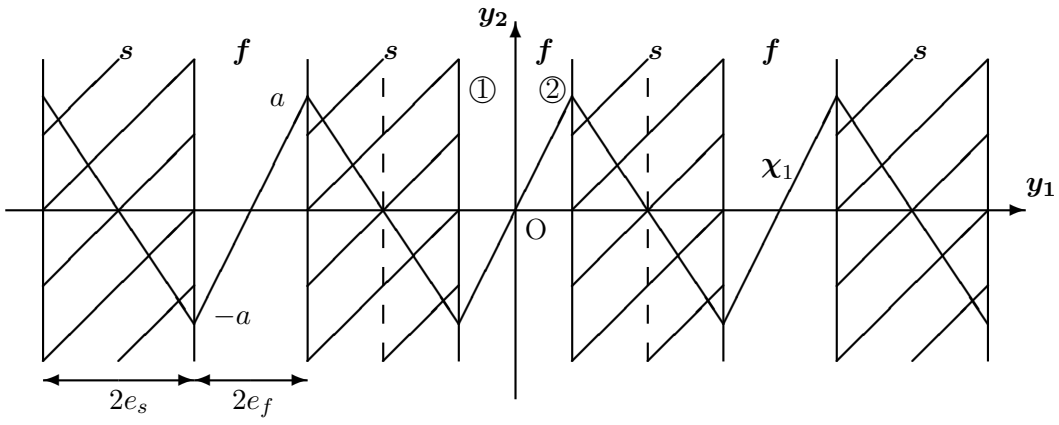

Figure A.5: Configuration of a periodic porous medium made of parallel solid and fluid layers

The closure problem in the unit-cell is written as

$$\left\{\begin{array}{rcll} 0 & = & \dfrac{\mathrm{d}}{\mathrm{d}y_1}\left(\lambda_f \dfrac{\mathrm{d}\chi_1^f}{\mathrm{d}y_1}\right) & -e_f < y_1 < e_f \\ 0 & = & \dfrac{\mathrm{d}}{\mathrm{d}y_1}\left(\lambda_s \dfrac{\mathrm{d}\chi_1^s}{\mathrm{d}y_1}\right) & -(e_f+e_{e_s}) < y_1 < -e_f \\ & & & e_f < y_1 < e_f+e_s \\ \chi_1^f & = & \chi_1^s & \text{at } y_1 = \pm e_f \\ \pm\lambda_s\left(\dfrac{\mathrm{d}\chi_1^s}{\mathrm{d}y_1}+1\right) & = & \pm\lambda_f\left(\dfrac{\mathrm{d}\chi_1^f}{\mathrm{d}y_1}+1\right) + 4\sigma {T^{(0)}}^3 \left(y_1+\beta_1-\{y_1+\beta_1\}_F\right) & \end{array}\right. \tag{A.1}$$

where the component β_1 is solution of the integral equation (25)

$$\beta_1 = \epsilon\chi_1 + (1-\epsilon)\left[\{y_1+\beta_1\}_F - y_1\right] \qquad y_1 = \pm e_f \tag{A.2}$$

χ_1 is determined by the problem (A.1) within a constant chosen to have a zero average. Eq. (A.1) shows that χ_1^f and χ_1^s vary linearly with y_1 and can be determined by the two extremities a and $-a$ at the solid/fluid interface (see Figure A.5). Let denote ① be the plane $y_1 = -e_f$ and ② be the plane $y_1 = e_f$. The view factors are $F_{11} = F_{22} = 0$ et $F_{12} = F_{21} = 1$. Hence, we have

$$\left\{\begin{array}{ll} \beta_1^{①} = -\epsilon(a+e_f) + (1-\epsilon)\left(\beta_1^{②} + 2e_f\right) & y_1 = -e_f \\ \beta_1^{②} = \epsilon(a+e_f) + (1-\epsilon)\left(\beta_1^{①} - 2e_f\right) & y_1 = e_f \end{array}\right. \tag{A.3}$$

leading to

$$\beta_1^{①} = -\beta_1^{②} = \frac{2(1-\epsilon)e_f - \epsilon a}{2-\epsilon} \tag{A.4}$$

$$\left(y_1+\beta_1-\{y_1+\beta_1\}_F\right)|^{①} = -\left(y_1+\beta_1-\{y_1+\beta_1\}_F\right)|^{②} = -\frac{2\epsilon}{2-\epsilon}(a+e_f) \tag{A.5}$$

The interface condition at $y_1 = \pm e_f$ is given as

$$-\lambda_s\left(1-\frac{a}{e_s}\right) = -\lambda_f\left(1+\frac{a}{e_f}\right) - 4\epsilon\sigma {T^{(0)}}^3 \frac{2(a+e_f)}{2-\epsilon} \tag{A.6}$$

leading to

$$a\left[\frac{4\epsilon\sigma {T^{(0)}}^3}{2-\epsilon} + \frac{\lambda_f}{2e_f} + \frac{\lambda_s}{2e_s}\right] = \frac{\lambda_s-\lambda_f}{2} - \frac{4\epsilon\sigma {T^{(0)}}^3 e_f}{2-\epsilon} \tag{A.7}$$

Denoting $\lambda_R/(2e_f) = 4\epsilon\sigma {T^{(0)}}^3/(2-\epsilon)$ gives

$$a\left[\frac{\lambda_f+\lambda_R}{2e_f} + \frac{\lambda_s}{2e_s}\right] = \frac{\lambda_s-(\lambda_f+\lambda_R)}{2} \tag{A.8}$$

The integral term in (34) is given as

$$\frac{1}{|Y_f|}\int_{\partial Y_{fs}} y_1\left(y_1+\beta_1-\{y_1+\beta_1\}_F\right)\mathrm{d}S = \left(y_1+\beta_1-\{y_1+\beta_1\}_F\right)|^{②} = \frac{2\epsilon}{2-\epsilon}(a+e_f) \tag{A.9}$$

Finally, the effective conductivity in the y_1 direction is obtained as

$$\begin{aligned}(\lambda_{eq})_{11} &= n_f\lambda_f\left(1+\frac{a}{e_f}\right)+n_s\lambda_s\left(1-\frac{a}{e_s}\right)+n_f 4\epsilon\sigma {T^{(0)}}^3\frac{2(a+e_f)}{2-\epsilon}\\ &= n_f\left(\lambda_f+\lambda_R\right)\left(1+\frac{a}{e_f}\right)+n_s\lambda_s\left(1-\frac{a}{e_s}\right)=\frac{1}{\dfrac{n_f}{\lambda_f+\lambda_R}+\dfrac{n_s}{\lambda_s}}\end{aligned} \tag{A.10}$$

which is an expected result.

Appendix A.2. Spherical pore

In the particular case of a spherical cavity of radius R the view factor is uniform on the sphere surface ($\mathrm{d}F_{\mathrm{d}S_1\to\mathrm{d}S_2} = \mathrm{d}S_2/(4\pi R^2)$) and therefore the view factor and the surface average are identical ($\{\ \}\equiv\{\ \}_F=\{\ \}_S$). Averaging relation (25) leads to $\{\boldsymbol{\beta}\}=\{\boldsymbol{\chi}\}$. Equation (25) can now be written

$$\mathbf{y}+\boldsymbol{\beta}-\{\mathbf{y}+\boldsymbol{\beta}\}=\epsilon\left[\mathbf{y}+\boldsymbol{\chi}-\{\mathbf{y}+\boldsymbol{\chi}\}\right]=\epsilon\left(R\,\mathbf{n}_f+\boldsymbol{\chi}-\{\boldsymbol{\chi}\}\right) \tag{A.11}$$

where R is the sphere radius and $\mathbf{n}_f$ the normal vector to the sphere. As noted before the result is independent of the origin of the coordinates $\mathbf{y}$ chosen here as the center of the spherical pore. Using relation (32), the radiative contribution to the equivalent conductivity is given by

$$\left\langle \mathbf{q}_f^{\mathrm{R}(0)}\right\rangle^f = -\frac{4\epsilon\sigma {T^{(0)}}^3}{|Y_f|}\int_{\partial Y_{fs}}\mathbf{y}\otimes\left(R\,\mathbf{n}_f+\boldsymbol{\chi}-\{\boldsymbol{\chi}\}\right)\mathrm{d}S\cdot\boldsymbol{\nabla}_x T^{(0)} \tag{A.12}$$

Using the following relations

$$R\int_{\partial Y_{fs}}\mathbf{y}\otimes\mathbf{n}_f\ \mathrm{d}S = R\int_{Y_f}\boldsymbol{I}\ \mathrm{d}V = R|Y_f|\boldsymbol{I} \tag{A.13}$$

$$\int_{\partial Y_{fs}}\mathbf{y}\otimes\boldsymbol{\chi}\ \mathrm{d}S = R\int_{\partial Y_{fs}}\mathbf{n}_f\otimes\boldsymbol{\chi}\,\mathrm{d}S = R\int_{Y_f}\boldsymbol{\nabla}_y\boldsymbol{\chi}_f\ \mathrm{d}V = R|Y_f|\left\langle\boldsymbol{\nabla}_y\boldsymbol{\chi}_f\right\rangle^f \tag{A.14}$$

$$\int_{\partial Y_{fs}}\mathbf{y}\otimes\{\boldsymbol{\chi}\}_S\ \mathrm{d}S = \left(\int_{\partial Y_{fs}}\mathbf{y}\ \mathrm{d}S\right)\otimes\{\boldsymbol{\chi}\}_S = 0 \tag{A.15}$$

the equivalent thermal conductivity is given by

$$\boldsymbol{\lambda}_{eq} = n_f\left(\lambda_f+4\epsilon\sigma {T^{(0)}}^3 R\right)\left(\boldsymbol{I}+\left\langle\boldsymbol{\nabla}_y\boldsymbol{\chi}_f\right\rangle^f\right)+n_s\lambda_s\left(\boldsymbol{I}+\left\langle\boldsymbol{\nabla}_y\boldsymbol{\chi}_s\right\rangle^s\right) \tag{A.16}$$

To conclude we consider the closure problem (27) to be solved for $\boldsymbol{\chi}_{f(s)}$. The boundary condition at the fluid-solid interface ∂Y_{fs} is written

$$-\lambda_f \mathbf{n}_f \cdot \left(\boldsymbol{I} + \boldsymbol{\nabla}_y \boldsymbol{\chi}_f\right) - \lambda_s \mathbf{n}_s \cdot \left(\boldsymbol{I} + \boldsymbol{\nabla}_y \boldsymbol{\chi}_s\right) = 4\epsilon\sigma {T^{(0)}}^3 \left(R\,\mathbf{n}_f + \boldsymbol{\chi}_f - \{\boldsymbol{\chi}_f\}\right) \quad \text{(A.17)}$$

Expanding in a Taylor series the vector $\boldsymbol{\chi}_f$ with respect to the sphere center, for a point on the surface of the sphere, it comes

$$\begin{array}{rcccccc} \boldsymbol{\chi}_f & = & \boldsymbol{\chi}_f(0) & + & R\,\mathbf{n}_f \cdot \boldsymbol{\nabla}_y \boldsymbol{\chi}_f(0) & + & \ldots \\ \{\boldsymbol{\chi}_f\} & = & \boldsymbol{\chi}_f(0) & & & + & \ldots \\ \boldsymbol{\chi}_f - \{\boldsymbol{\chi}_f\} & = & & & R\,\mathbf{n}_f \cdot \boldsymbol{\nabla}_y \boldsymbol{\chi}_f(0) & + & \ldots \end{array} \quad \text{(A.18)}$$

If the gradient of $\boldsymbol{\chi}_f$ is assumed to be nearly uniform within the sphere, the interface condition is written:

$$-\left(\lambda_f + 4\epsilon\sigma {T^{(0)}}^3 R\right) \mathbf{n}_f \cdot \left(\boldsymbol{I} + \boldsymbol{\nabla}_y \boldsymbol{\chi}_f\right) - \lambda_s \mathbf{n}_s \cdot \left(\boldsymbol{I} + \boldsymbol{\nabla}_y \boldsymbol{\chi}_s\right) \simeq 0 \quad \text{(A.19)}$$

Note that the hypothesis of a constant temperature gradient inside the inclusion is the key of the effective-medium approximations based on the single inclusion problem [40]. In the case of a spherical pore, taking into account the radiation in the cavities is equivalent to adding to the thermal conductivity of the fluid λ_f a radiative contribution equal to $4\epsilon\sigma {T^{(0)}}^3 R$. This good approximation allows the use of standard methods to evaluate the equivalent thermal conductivity of the medium in a simple way.

Appendix B. Effective coefficients in cylindrical pore geometry

In this appendix, the calculation of the effective conductivity in the case of a cylindrical pore geometry is detailed.

Appendix B.1. Problem in $\boldsymbol{\beta}$

The problem (52) has to be solved with $\boldsymbol{\beta}$ defined on the surface element $\mathrm{d}S(y_1) = r_0 \mathrm{d}\theta \mathrm{d}y_1$ where $S(y_1)$ is the lateral surface of the cylinder at the abscissa y_1 and θ the polar angle in the plane Oy_2y_3. First in the section of the origin frame, we have

$$\begin{aligned} \{\boldsymbol{\beta} + \mathbf{y}\}_F &= \int_{y_1=-\infty}^{+\infty} \int_{\theta=0}^{2\pi} \mathrm{d}F_{\mathrm{d}S(0)\to\mathrm{d}S(y_1)} \left[\beta_1\, \widehat{\mathbf{e}}_1 + (\beta_r + r_0)\, \widehat{\mathbf{e}}_r\right] \\ &= \beta_1 \widehat{\mathbf{e}}_1 + \underbrace{2\int_{y_1=0}^{+\infty} \int_{\theta=0}^{2\pi} \mathrm{d}F_{\mathrm{d}S(0)\to\mathrm{d}S(y_1)} (\beta_r + r_0)\, \widehat{\mathbf{e}}_r}_{\{(\beta_r + r_0)\, \widehat{\mathbf{e}}_r\}_F} \end{aligned} \quad \text{(B.1)}$$

The quantity $\{(\beta_r + r_0)\ \widehat{\mathbf{e}}_r\}_F$ independent on θ is determined at point A of coordinates $(0, r_0, 0)$ while the current point B belonging to $S(y_1)$ has the coordinates $(y_1, r_0\cos\theta, r_0\sin\theta)$ $(0 < \theta < 2\pi)$. The vector $\overrightarrow{AB}$ is given by

$$\overrightarrow{AB} = \begin{pmatrix} y_1 \\ r_0(\cos\theta - 1) \\ r_0\ \sin\theta \end{pmatrix}; \quad \mathbf{n}_A = \begin{pmatrix} 0 \\ -1 \\ 0 \end{pmatrix}; \quad \mathbf{n}_B = \begin{pmatrix} 0 \\ -\cos\theta \\ -\sin\theta \end{pmatrix} \tag{B.2}$$

$$\|AB\|^2 = y_1^2 + 2r_0^2\,(1 - \cos\theta) = y_1^2 + 4r_0^2\sin^2(\theta/2) \tag{B.3}$$

$$\cos\theta_A = \frac{\overrightarrow{AB}\cdot\mathbf{n}_A}{\|AB\|} = \frac{2r_0\sin^2(\theta/2)}{\|AB\|} \tag{B.4}$$

$$\cos\theta_B = \frac{\overrightarrow{BA}\cdot\mathbf{n}_B}{\|AB\|} = \frac{r_0(1-\cos\theta)}{\|AB\|} = \frac{2r_0\sin^2(\theta/2)}{\|AB\|} \tag{B.5}$$

445 The view factor is written as

$$\mathrm{d}F_{\mathrm{d}S(0)\to\mathrm{d}S(y_1)} = \Omega_{\mathrm{d}S(0)\to\mathrm{d}S(y_1)}\mathrm{d}S(y_1) \tag{B.6}$$

$$\Omega_{\mathrm{d}S(0)\to\mathrm{d}S(y_1)} = \frac{\cos\theta_A\ \cos\theta_B}{\pi\|AB\|^2} = \frac{4r_0^2\sin^4(\theta/2)}{\pi\left(y_1^2 + 4r_0^2\sin^2(\theta/2)\right)^2} \tag{B.7}$$

Hence, we have

$$\begin{aligned}
\{(\beta_r + r_0)\ \widehat{\mathbf{e}}_r\}_F &= \int_{-\infty}^{\infty}\mathrm{d}y_1\int_0^{2\pi}\frac{4r_0^2\sin^4(\theta/2)}{\pi\left(y_1^2 + 4r_0^2\sin^2(\theta/2)\right)^2}(\beta_r + r_0)\begin{pmatrix} 0 \\ \cos\theta \\ \sin\theta \end{pmatrix} r_0\ \mathrm{d}\theta \\
&= \int_0^{2\pi}\frac{4r_0^2\sin^4(\theta/2)}{2\left(2r_0\sin(\theta/2)\right)^3}(\beta_r + r_0)\begin{pmatrix} 0 \\ \cos\theta \\ \sin\theta \end{pmatrix} r_0\ \mathrm{d}\theta \\
&= \frac{1}{4}\int_0^{2\pi}\sin(\theta/2)\,(\beta_r + r_0)\begin{pmatrix} 0 \\ \cos\theta \\ \sin\theta \end{pmatrix}\mathrm{d}\theta = -(\beta_r + r_0)\,\frac{\widehat{\mathbf{e}}_r}{3}
\end{aligned} \tag{B.8}$$

Eq. (52) is now written as

$$\begin{aligned}
\boldsymbol{\beta} &= \epsilon\,\boldsymbol{\chi} + (1-\epsilon)\,(\{\mathbf{y} + \boldsymbol{\beta}\}_F - \mathbf{y}) \\
\beta_1\widehat{\mathbf{e}}_1 + \beta_r\,\widehat{\mathbf{e}}_r &= \epsilon\,[\chi_1(r_0)\,\widehat{\mathbf{e}}_1 + \chi_r(r_0)\,\widehat{\mathbf{e}}_r] + (1-\epsilon)\left[\beta_1\widehat{\mathbf{e}}_1 - (\beta_r + r_0)\,\frac{\widehat{\mathbf{e}}_r}{3} - r_0\widehat{\mathbf{e}}_r\right]
\end{aligned} \tag{B.9}$$

Therefore

$$\begin{aligned} \beta_1 &= \chi_1(r_0) \\ \beta_r &= \frac{3}{4-\epsilon}\left[\epsilon\chi_r(r_0) - \frac{4}{3}(1-\epsilon)r_0\right] \\ \mathbf{y}+\boldsymbol{\beta}-\{\mathbf{y}+\boldsymbol{\beta}\}_F &= \frac{4\epsilon}{4-\epsilon}\left[r_0+\chi_r(r_0)\right]\widehat{\mathbf{e}}_r \end{aligned} \tag{B.10}$$

Appendix B.2. Problem in $\boldsymbol{\chi}$

The problem to be solved in $\boldsymbol{\chi}$ is given by

$$\left\{\begin{array}{rcll} \mathbf{v}_f\cdot\boldsymbol{\nabla}_y\boldsymbol{\chi}_f &=& \dfrac{\lambda_f}{(\rho c)_f}\nabla_y^2\boldsymbol{\chi}_f+\gamma_f\left\langle\mathbf{v}_f\right\rangle^f-\mathbf{v}_f & \text{in } Y_f \\ 0 &=& \dfrac{\lambda_s}{(\rho c)_s}\nabla_y^2\boldsymbol{\chi}_s+\gamma_f\left\langle\mathbf{v}_f\right\rangle^f & \text{in } Y_s \\ \boldsymbol{\chi}_f &=& \boldsymbol{\chi}_s & \\ -\mathbf{n}_f\cdot\lambda_f\left(\boldsymbol{I}+\boldsymbol{\nabla}_y\boldsymbol{\chi}_f\right) & & & \Big\} \text{ on } \partial Y_{fs} \\ -\mathbf{n}_s\cdot\lambda_s\left(\boldsymbol{I}+\boldsymbol{\nabla}_y\boldsymbol{\chi}_s\right) &=& 4\sigma{T^{(0)}}^3\left(\mathbf{y}+\boldsymbol{\beta}-\{\mathbf{y}+\boldsymbol{\beta}\}_F\right) & \end{array}\right. \tag{B.11}$$

where the velocity profile obeys a Poiseuille law $\mathbf{v}_f = 2\left\langle v\right\rangle^f\left[1-\left(\dfrac{r}{r_0}\right)^2\right]\widehat{\mathbf{e}}_1$ and the vector $\mathbf{y}+\boldsymbol{\beta}-\{\mathbf{y}+\boldsymbol{\beta}\}_F$ is given by relation (B.10). The uniqueness of the problem in $\boldsymbol{\chi}$ is ensured by condition (76).

The solution of $\boldsymbol{\chi}_{f(s)}(r)$ in the fluid phase (or in the solid phase) is sought in the form

$$\boldsymbol{\chi}_{f(s)}(r) = \chi_1^{f(s)}(r)\,\widehat{\mathbf{e}}_1 + \chi_r^{f(s)}(r)\,\widehat{\mathbf{e}}_r \tag{B.12}$$

Appendix B.2.1. Problem in $\chi_1^{f(s)}(r)$

The problem (75) in $\chi_1(r)$ is written:

$$\left\{\begin{array}{rcll} 0 &=& \dfrac{1}{r}\dfrac{\mathrm{d}}{\mathrm{d}r}\left(r\dfrac{\mathrm{d}\chi_1^f}{\mathrm{d}r}\right)+\dfrac{\left\langle v_f\right\rangle^f}{a_f}\left[\gamma_f-2+2\left(\dfrac{r}{r_0}\right)^2\right] & 0<r<r_0 \\ 0 &=& \dfrac{1}{r}\dfrac{\mathrm{d}}{\mathrm{d}r}\left(r\dfrac{\mathrm{d}\chi_1^s}{\mathrm{d}r}\right)+\gamma_f\dfrac{\left\langle v_f\right\rangle^f}{a_s} & r_0<r<r_1 \\ \chi_1^f &=& \chi_1^s & r=r_0 \\ \lambda_f\dfrac{\mathrm{d}\chi_1^f}{\mathrm{d}r} &=& \lambda_s\dfrac{\mathrm{d}\chi_1^s}{\mathrm{d}r} & \\ 0 &=& (\rho c)_f\left\langle\chi_1^f\right\rangle^f+(\rho c)_s\left\langle\chi_1^s\right\rangle^s & \end{array}\right. \tag{B.13}$$

We obtain the following solution

$$\left\langle \chi_1^f \right\rangle^f = (1-\gamma_f)\langle v_f\rangle^f r_0^2 \left[\frac{1}{a_f}\left(\frac{\gamma_f}{8}-\frac{1}{6}\right)+\frac{\gamma_f}{a_s}\left(-\frac{1}{8}+\frac{3}{8n_f}+\frac{\log n_f}{4n_f(1-n_f)}\right)\right] \quad \text{(B.14)}$$

$$\langle \chi_1^s \rangle^s = -\gamma_f \langle v_f\rangle^f r_0^2 \left[\frac{1}{a_f}\left(\frac{\gamma_f}{8}-\frac{1}{6}\right)+\frac{\gamma_f}{a_s}\left(-\frac{1}{8}+\frac{3}{8n_f}+\frac{\log n_f}{4n_f(1-n_f)}\right)\right] \quad \text{(B.15)}$$

with $\gamma_f = n_f(\rho c)_f/\langle \rho c\rangle$. The longitudinal component of $\mathbf{\Lambda}_{disp}$ given by equation (84) is equal to:

$$-n_f(\rho c)_f \left\langle v_f \chi_1^f \right\rangle^f = n_f \lambda_f \left(\frac{\langle v_f\rangle^f r_0}{a_f}\right)^2 \left[\frac{6\gamma_f^2-16\gamma_f+11}{48}+\frac{(\rho c)_f(\rho c)_s}{\langle \rho c\rangle^2}\frac{a_f}{a_s}\left(-3-2\log n_f+4n_f-n_f^2\right)\right] \quad \text{(B.16)}$$

Note that if $n_f = 1$ (and therefore $\gamma_f = 1$), the dispersion coefficient becomes $\lambda_f \mathrm{Pe}^2/48$ with $\mathrm{Pe} = \langle v_f\rangle^f r_0/a_f$, which is an expected result.

Appendix B.2.2. Problem in $\chi_r^{f(s)}(r)$

The problem (B.11) is now solved for the function $\chi_r(r)\widehat{\mathbf{e}}_r$ which satisfies the following differential equation:

$$\chi_r'' + \frac{\chi_r'}{r} - \frac{\chi_r}{r^2} = 0 \quad \text{(B.17)}$$

where the symbol ' indicates a derivation with respect to r. The solution of problem (B.17) for $\chi_r^{f(s)}$ in the fluid (or the solid) phase reads as

$$\begin{cases} \chi_r^f = C\,r & 0 < r < r_0 \\ \chi_r^s = \dfrac{A}{r} + Br & r_0 < r < r_1 \end{cases} \quad \text{(B.18)}$$

The transmission conditions at $r = r_0$ are given by

$$\chi_r^f = \chi_r^s \quad \text{(B.19)}$$

$$-\lambda_f\left(1+(\chi_r^f)'\right) = -\lambda_s\left(1+(\chi_r^s)'\right) + \frac{16\epsilon\sigma {T^{(0)}}^3 r_0}{4-\epsilon}\left(1+\frac{\chi_r^f}{r_0}\right) \quad \text{(B.20)}$$

As χ_r^f is proportional to r, the condition for the flux at $r = r_0$ can be written:

$$-\lambda_f^*\left(1+(\chi_r^f)'\right) = -\lambda_s\left(1+(\chi_r^s)'\right) \quad \text{(B.21)}$$

with $\lambda_f^* = \lambda_f + \dfrac{16\epsilon\sigma {T^{(0)}}^3 r_0}{4-\epsilon}$. Since χ_r is supported by the vector $\widehat{\mathbf{e}}_r$, periodicity at the cell frontier ($r = r_1$) requires that

$$\chi_r^s(r=r_1) = \frac{A}{r_1} + Br_1 = 0 \quad \text{(B.22)}$$

Note that the tensor $\boldsymbol{\nabla\chi}^s$ is identical at two diametrically opposed points, thus ensuring the periodic condition for the flux. From the three relations (B.19-B.22), the coefficients B, C can be determined:

$$\left\{\begin{array}{rcl} B &=& \dfrac{n_f\left(\lambda_f^*-\lambda_s\right)}{(1-n_f)\lambda_f^*+(1+n_f)\lambda_s} \\ C &=& -B\dfrac{1-n_f}{n_f}=\dfrac{(1-n_f)\left(\lambda_s-\lambda_f^*\right)}{(1-n_f)\lambda_f^*+(1+n_f)\lambda_s} \end{array}\right. \tag{B.23}$$

with $n_f = r_0^2/r_1^2$. β_r is given by

$$r_0+\beta_r = \frac{3\epsilon}{4-\epsilon}\left(r_0+\chi_r(r_0)\right) = \frac{3\epsilon r_0}{4-\epsilon}\left(1+C\right) \tag{B.24}$$

Working in the 2D (Oy_2y_3) space perpendicular to the axis Oy_1, the average gradients in the fluid and solid phases are given by:

$$\left\langle\, \boldsymbol{\nabla\chi}_f\big|_{2\mathrm{D}} \,\right\rangle^f = \frac{1}{r_0^2}\int_0^{r_0}\left(r\chi_f'+\chi_f\right)\mathrm{d}r\ \boldsymbol{I}_{2\mathrm{D}} = C\,\boldsymbol{I}_{2\mathrm{D}} \tag{B.25}$$

$$\left\langle\, \boldsymbol{\nabla\chi}_s|_{2\mathrm{D}} \,\right\rangle^s = \frac{1}{r_1^2-r_0^2}\int_{r_0}^{r_1}\left(r\chi_s'+\chi_s\right)\mathrm{d}r\ \boldsymbol{I}_{2\mathrm{D}} = B\,\boldsymbol{I}_{2\mathrm{D}} \tag{B.26}$$

where $\boldsymbol{I}_{2\mathrm{D}}$ is the 2D unit tensor. To compute the effective conductivity $\lambda_{2\mathrm{D}}^{eff}$ in the transverse direction, the integral part of the radiative conductivity (63) acting in the transverse direction has to be added, leading to

$$\lambda_{2\mathrm{D}}^{eff}\boldsymbol{I}_{2\mathrm{D}} = n_f\left[\lambda_f\left(\boldsymbol{I}_{2\mathrm{D}}+\left\langle\, \boldsymbol{\nabla\chi}_f\big|_{2\mathrm{D}} \,\right\rangle^f\right)+\frac{4\sigma {T^{(0)}}^3}{|Y_f|}\int_{\partial Y_{fs}}\mathbf{y}\otimes\left(\mathbf{y}+\boldsymbol{\beta}-\{\mathbf{y}+\boldsymbol{\beta}\}_F\right)\mathrm{d}S\right] \tag{B.27}$$

$$+\ n_s\lambda_s\left(\boldsymbol{I}_{2\mathrm{D}}+\langle\, \boldsymbol{\nabla\chi}_s|_{2\mathrm{D}}\rangle^s\right) \tag{B.28}$$

The calculation of the radiative part of the conductivity is easy using relation (B.10) and (B.24):

$$\frac{1}{|Y_f|}\int_{\partial Y_{fs}}\mathbf{y}\otimes\left(\mathbf{y}+\boldsymbol{\beta}-\{\mathbf{y}+\boldsymbol{\beta}\}_F\right)\mathrm{d}S = \frac{4}{3}\left(r_0+\beta_r\right)\boldsymbol{I}_{2\mathrm{D}} = \frac{4\epsilon r_0}{4-\epsilon}(1+C)\boldsymbol{I}_{2\mathrm{D}} \tag{B.29}$$

From Equation. (B.24) and (B.25)

$$\lambda_f\left(\boldsymbol{I}_{2\mathrm{D}}+\left\langle\, \boldsymbol{\nabla\chi}_f\big|_{2\mathrm{D}} \,\right\rangle^f\right) = \lambda_f(1+C)\boldsymbol{I}_{2\mathrm{D}} \tag{B.30}$$

$$\lambda_f\left(\boldsymbol{I}_{2\mathrm{D}}+\left\langle\, \boldsymbol{\nabla\chi}_f\big|_{2\mathrm{D}} \,\right\rangle^f\right)+\frac{4\sigma {T^{(0)}}^3}{|Y_f|}\int_{\partial Y_{fs}}\mathbf{y}\otimes\left(\mathbf{y}+\boldsymbol{\beta}-\{\mathbf{y}+\boldsymbol{\beta}\}_F\right)\mathrm{d}S$$
$$=\lambda_f^*\left(\boldsymbol{I}_{2\mathrm{D}}+\left\langle\, \boldsymbol{\nabla\chi}_f\big|_{2\mathrm{D}} \,\right\rangle^f\right) \tag{B.31}$$

The conductivity in the plane perpendicular to the cylinder axis using (B.23) is finally given by

$$\lambda_{\rm 2D}^{eff} \quad = \quad n_f\lambda_f^*(1+C)+n_s\lambda_s(1+B)=\lambda_s\,\frac{(1+n_f)\lambda_f^*+(1-n_f)\lambda_s}{(1-n_f)\lambda_f^*+(1+n_f)\lambda_s} \tag{B.32}$$

with $\lambda_f^*=\lambda_f+\dfrac{16\epsilon\sigma {T^{(0)}}^3 r_0}{4-\epsilon}$. This two-dimensional problem for a continuous phase of conductivity λ_s and a dispersed phase of conductivity λ_f^* is similar to the 2D conductive homogenization known as Maxwell's formula [39, 40].

Appendix B.3. Radiative flux in the longitudinal direction

The radial part of the conductivity (63) has already been calculated. For the second term $\boldsymbol{\alpha}$, only the component $\boldsymbol{\alpha}^1$ is non-null and given by

$$\boldsymbol{\alpha}^1=\frac{1}{\ell_2\ell_3}\sum_{\substack{\mathbf{k}\,\in\,\mathbb{Z}^3\\ k_1<0}}\sum_{\substack{\mathbf{m}\,\in\,\mathbb{Z}^3\\ m_1\geq 0}}\left[\int_{\mathcal{S}_{\{\mathbf{k}\}}}\int_{\mathcal{S}_{\{\mathbf{m}\}}}\left[\boldsymbol{L}\cdot(\mathbf{m}-\mathbf{k})\right]\mathrm{d}S_{\{\mathbf{k}\}}\mathrm{d}F_{\mathrm{d}S_{\{\mathbf{k}\}}\to\mathrm{d}S_{\{\mathbf{m}\}}}\right] \tag{B.33}$$

which is a longitudinal vector, $\boldsymbol{\alpha}^1=\alpha^1\,\widehat{\mathbf{e}}_1$. To simplify the notations, y designates the coordinate y_1, the coordinates in the plane perpendicular to the cylinder axis are represented using polar coordinates with radius r and angle θ. The view factor between two annular elements $\mathrm{d}S_1$ and $\mathrm{d}S_2$ is equal to the view factor from a current point 1 of the surface ($\theta_1=0$) with the annular element $\mathrm{d}S_2$ at distance $y=|y_2-y_1|$ of width $\mathrm{d}y_2$.

$$\begin{aligned}\mathrm{d}F_{\mathrm{d}S_1\to\mathrm{d}S_2} \quad &= \quad \mathrm{d}F_{1\to\mathrm{d}S_2}=\int_{\theta_2=0}^{2\pi}\Omega_{12}\,r_0\,\mathrm{d}\theta_2\mathrm{d}y_2\\ &= \quad \left(1-\frac{3Y+2Y^3}{2\,(1+Y^2)}\right)\mathrm{d}Y_2 \qquad \text{with} \quad Y=\frac{|y_2-y_1|}{2r_0}\end{aligned} \tag{B.34}$$

We can have

$$\alpha^1 \quad = \quad \frac{1}{\pi r_1^2}\int_{y_1=-\infty}^{0}2\pi r_0\mathrm{d}y_1\int_{y_2=0}^{\infty}(y_2-y_1)\,\mathrm{d}F_{\mathrm{d}S_1\to\mathrm{d}S_2}=\frac{8\pi r_0^3}{3\pi r_1^2}=n_f\frac{8r_0}{3} \tag{B.35}$$

Finally, the average radiative conductivity in the longitudinal direction reads as

$$\boldsymbol{\lambda}^{\mathrm{R}}\Big|_{11}=\frac{32n_f\,\epsilon\,\sigma {T^{(0)}}^3 r_0}{3} \tag{B.36}$$

References

[1] T. Fend, B. Hoffschmidt, R. Pitz-Paal, O. Reutter, P. Rietbrock, Porous materials as open volumetric solar receivers: Experimental determination of thermophysical and heat transfer properties, Energy 29 (5-6) (2004) 823–833. doi:10.1016/S0360-5442(03)00188-9.

[2] E. Velasco GÃmez, F. Rey MartÃnez, F. Varela Diez, M. Molina Leyva, R. Herrero MartÃn, Description and experimental results of a semi-indirect ceramic evaporative cooler, International Journal of Refrigeration 28 (5) (2005) 654–662. doi:10.1016/j.ijrefrig.2005.01.004.

[3] E. Jahanshahi Javaran, S. Gandjalikhan Nassab, S. Jafari, Thermal analysis of a 2-D heat recovery system using porous media including lattice Boltzmann simulation of fluid flow, International Journal of Thermal Sciences 49 (6) (2010) 1031–1041. doi:10.1016/j.ijthermalsci.2009.12.004.

[4] J. Randrianalisoa, Y. BrÃ©chet, D. Baillis, Materials Selection for Optimal Design of a Porous Radiant Burner for Environmentally Driven Requirements, Advanced Engineering Materials (Jul. 2009). doi:10.1002/adem.200900089.

[5] R. Coquard, D. Baillis, Modeling of Heat Transfer in Low-Density EPS Foams, Journal of Heat Transfer 128 (6) (2006) 538. doi:10.1115/1.2188464.

[6] J. M. Chavez, C. Chaza, Testing of a porous ceramic absorber for a volumetric air receiver, Solar Energy Materials 24 (1-4) (1991) 172–181.

[7] P. Ranut, On the effective thermal conductivity of aluminum metal foams: Review and improvement of the available empirical and analytical models, Applied Thermal Engineering 101 (2016) 496–524. doi:10.1016/j.applthermaleng.2015.09.094.

[8] M. N. Miller, Bounds for Effective Electrical, Thermal, and Magnetic Properties of Heterogeneous Materials, Journal of Mathematical Physics 10 (11) (1969) 1988–2004. doi:10.1063/1.1664794.

[9] Z. Hashin, S. Shtrikman, A Variational Approach to the Theory of the Effective Magnetic Permeability of Multiphase Materials, Journal of Applied Physics 33 (10) (1962) 3125–3131. doi:10.1063/1.1728579.

[10] J. W. Paek, B. H. Kang, S. Y. Kim, J. M. Hyun, Effective thermal conductivity and permeability of aluminum foam materials, International Journal of Thermophysics 21 (2) (2000) 453–464.

[11] K. Boomsma, D. Poulikakos, On the effective thermal conductivity of a three-dimensionally structured fluid-saturated metal foam, International Journal of Heat and Mass Transfer 44 (4) (2001) 827–836.

[12] V. V. Calmidi, R. L. Mahajan, The effective thermal conductivity of high porosity fibrous metal foams, Journal of Heat Transfer 121 (2) (1999).

[13] A. Bhattacharya, V. Calmidi, R. Mahajan, Thermophysical properties of high porosity metal foams, International Journal of Heat and Mass Transfer 45 (5) (2002) 1017–1031.

[14] R. Wulf, M. A. A. Mendes, V. Skibina, A. Al-Zoubi, D. Trimis, S. Ray, U. Gross, Experimental and numerical determination of effective thermal conductivity of open cell fecral-alloy metal foams, International Journal of Thermal Sciences 86 (2014) 95–103.

[15] R. Coquard, D. Rochais, D. Baillis, Experimental investigations of the coupled conductive and radiative heat transfer in metallic/ceramic foams, International Journal of Heat and Mass Transfer 52 (21-22) (2009) 4907–4918. doi:10.1016/j.ijheatmasstransfer.2009.05.015.

[16] S. Cunsolo, R. Coquard, D. Baillis, N. Bianco, Radiative properties modeling of open cell solid foam: Review and new analytical law, International Journal of Thermal Sciences 104 (2016) 122–134. doi:10.1016/j.ijthermalsci.2015.12.017.

[17] B. Zeghondy, E. Iacona, J. Taine, Determination of the anisotropic radiative properties of a porous material by radiative distribution function identification (RDFI), International Journal of Heat and Mass Transfer 49 (17-18) (2006) 2810–2819. doi:10.1016/j.ijheatmasstransfer.2006.02.034.

[18] M. A. Badri, P. Jolivet, B. Rousseau, S. Le Corre, H. Digonnet, Y. Favennec, Vectorial finite elements for solving the radiative transfer equation, Journal of Quantitative Spectroscopy and Radiative Transfer 212 (2018) 59 – 74.

[19] L. Ibarrart, C. Caliot, M. El Hafi, R. Fournier, S. Blanco, S. Dutour, J. Dauchet, J.-M. Tregan, V. Eymet, V. Forest, Combined conductive-convective-radiative heat transfer in complex geometry using the monte carlo method : Application to solar receivers, in: International Heat Transfer Conference 16, Begellhouse, Beijing, China, 2018, pp. 8135–8142. doi:10.1615/IHTC16.pma.023662.

[20] M. A. A. Mendes, V. Skibina, P. Talukdar, R. Wulf, U. Gross, D. Trimis, S. Ray, Experimental validation of simplified conduction–radiation models for evaluation of effective thermal conductivity of open-cell metal foams at high temperatures, International Journal of Heat and Mass Transfer 78 (2014) 112–120.

[21] M. A. A. Mendes, P. Talukdar, S. Ray, D. Trimis, Detailed and simplified models for evaluation of effective thermal conductivity of open-cell porous foams at high temperatures in presence of thermal radiation, International Journal of Heat and Mass Transfer 68 (2014) 612–624.

[22] V. M. Patel, M. A. A. Mendes, P. Talukdar, S. Ray, Development of correlations for effective thermal conductivity of a tetrakaidecahedra structure in presence of combined conduction and radiation heat transfer, International Journal of Heat and Mass Transfer 127 (2018) 843–856.

[23] G. L. Vignoles, A hybrid random walk method for the simulation of coupled conduction and linearized radiation transfer at local scale in porous media with opaque solid phases, International Journal of Heat and Mass Transfer 93 (2016) 707–719.

[24] M. Sans-Laurent, O. Farges, V. Schick, C. Moyne, G. Parent, Modeling the Flash Method by using a Conducto-Radiative Monte-Carlo Method: Application to Porous Media, in: 9th International Symposium on Radiative Transfer (RAD-19), Proceedings of the 9th International Symposium on Radiative Transfer, RAD-19, Begellhouse, Athènes, Greece, 2019, pp. 319–326. doi:10.1615/RAD-19.390.

[25] M. Luo, C. Wang, J. Zhao, L. Liu, Characteristics of effective thermal conductivity of porous materials considering thermal radiation: A pore-level analysis, International Journal of Heat and Mass Transfer 188 (2022) 122597.

[26] B. Fiers, G. Ferschneider, D. Maillet, Reduced model for characterization of solid wall effects for transient thermal dispersion in granular porous media, International Journal of Heat and Mass Transfer 53 (25-26) (2010) 5962–5975.

[27] A. Testu, S. Didierjean, D. Maillet, C. Moyne, T. Metzger, T. Niass, Thermal dispersion for water or air flow through a bed of glass beads, International Journal of Heat and Mass Transfer 50 (7-8) (2007) 1469–1484.

[28] D. Edouard, T. T. Huu, C. P. Huu, F. Luck, D. Schweich, The effective thermal properties of solid foam beds: Experimental and estimated temperature profiles, International Journal of Heat and Mass Transfer 53 (19-20) (2010) 3807–3816.

[29] C. Hutter, A. Zenklusen, R. Lang, P. R. von Rohr, Axial dispersion in metal foams and streamwise-periodic porous media, Chemical engineering science 66 (6) (2011) 1132–1141.

[30] H. Xu, Z. Xing, F. Wang, Z. Cheng, Review on heat conduction, heat convection, thermal radiation and phase change heat transfer of nanofluids in porous media: Fundamentals and applications, Chemical Engineering Science 195 (2019) 462–483.

[31] Z. Wu, C. Caliot, G. Flamant, Z. Wang, Coupled radiation and flow modeling in ceramic foam volumetric solar air receivers, Solar Energy 85 (9) (2011) 2374–2385. doi:10.1016/j.solener.2011.06.030.

[32] J. Ma, Y. Sun, B. Li, Simulation of combined conductive, convective and radiative heat transfer in moving irregular porous fins by spectral element method, International Journal of Thermal Sciences 118 (2017) 475–487.

[33] C. Moyne, S. Didierjean, H. P. A. Souto, O. T. Da Silveira, Thermal dispersion in porous media: one-equation model, International Journal of Heat and Mass Transfer 43 (20) (2000) 3853–3867.

[34] S. Whitaker, Radiant energy transport in porous media, Ind. Eng. Chem. Fundam. 19 (20) (1980) 210–219.

[35] J.-L. Auriault, A. P. M., Taylor dispersion in porous media: analysis by multiple scale expansions, Advances in Water Resources 18 (4) (1995) 217–226.

[36] T. Levy, Filtration in a porous fissured rock: influence of the fissures connexity, European Journal of Mechanics - B/Fluids 9 (1990) 309â327.

[37] J. Lewandowska, J.-L. Auriault, Modelling of unsaturated water flow in soils with highly permeable inclusions, C. R. Mecanique 332 (2004) 91â“96.

[38] G. Allaire, R. Brizzi, A. Mikelic, A. Piatnitski, Two-scale expansion with drift approach to the taylor dispersion for reactive transport through porous media, Chemical Engineering Science 65 (7) (2010) 2292–2300.

[39] H.-C. Chang, Multiscale analysis of effective transport in periodic heterogeneous media, Chem. Eng. Commun. 15 (4) (1982) 83–91.

[40] S. Torquato, Random Heterogeneous Materials: Microstructure and Macroscopic Properties, Springer, 2002.